ADDIS ABABA UNIVERSITY

ADDIS ABABA INSTITUTE OF TECNOLOGY

SCHOOLOF MECHNICAL AND INDUSTRIAL ENGINEERING

INFLUENCES OF MATERIAL ON SURFACE DAMAGE AT WHEEL- RAIL CONTACT

BY

Wudie Dagnew

A Thesis Submitted to the School of Graduate Studies of Addis Ababa University in Partial Fulfillment of the Requirements for the Degree of Masters of Science in Mechanical Engineering (Railway stream)

Advisor

Dr. Daniel Tilahun

June, 2016

Addis Ababa Institute of Technology (AAIT)
School of Mechanical & Industrial Engineering
Railway Engineering

INFLUNCES OF MATERIAL ON SURFACE DAMGE AT WHEEL/RAIL CONTACT

By
Wudie Dagnew

Approved by Board of Examining

Dr. Birhanu Beshah ________________________
Railway Centre Head

Dr. Daniel Tilahun ____________________
Advisor

Mr. Tsegaye Feleke ____________________
Internal Examiner

Mr. Habtamu Tikubet ____________________
External Examiner

DECLARATION

I here by declare that the work which is being presented in this thesis entitled ‘ INFLUNCES OF MATERIAL ON SURFACE DAMGE AT WHEEL/RAIL CONTACT’’ is original work of my own, has not been presented for a degree of any other university and all the resource materials used for this thesis have been duly acknowledged.

______________________ Wudie Dagnew

_____________ Date

This is to certify that the above declaration made by the candidate is correct to the best of my knowledge.

______________________ Dr. Daniel Tilahun (Advisor)

_____________ Date

ACKNOWLEDGMENT

First and for most, I would like to give my magnificence and respect to the Almighty GOD for his giving me strength, patience, invaluable cares and support throughout the course of my life and completion of this work, and frontward too.

Next, I would like to express deepest gratitude to my advisor Dr .Daniel Tilahun for his constant motivation, guidance, support, supervision and constructive suggestion throughout this thesis work. I would also like to thank Mr Dawit(Msc) , staff of Ethiopia Railways Corporation, for providing me with the necessary data which are used in the development of the thesis

I extend my sense of gratitude to all my friends who directly or indirectly help me in this end eavor

I also would like to thank my friends wubneh tefera for the invaluable support and patience during the research work. My thanks also go to my beloved family for their moral support, without them I would not be where I am right now

ABSTRACT

The paper will study the influence of material on surface damage on the wheel - rail materials The study begins with identifying basic criteria to select an appropriate steel materials for wheel and rail among different alternatives. The basic criteria are cost, material compositions, mechanical properties such as tensile strength, proof load, fatigue strength, toughness by using the criteria two pair of wheel- rail material selected (AS4140-V1657) and (C74-U75V) comparing with AALRT wheel - rail material (CL60&U71MN)

Next analyzing and identifying the stresses on the wheel –rail contact due to the load to predict and minimize failures caused. the 3D model has done on modeling package of CATIAV5R16. Assembly model has created in assemble workbench of CATIA after individual wheel and rail had created on part work bench after the assembly is accomplished on CATIA. it was imported in to the ANSYSR14.5 to analyze the stress caused by vertical load. During the analysis of wheel/rail contact in ANSYS software, the parameters have been used axle load, displacement, heat fulx, heat convection.

From ANSYS software simulation the results obtained for the one wheels-rail contact show that, (AS4140&V1657) has excellent strength, toughness and good resistance to thermal damage due to better hardness than (CL60-U71MN) &(C74&U75V). Therefore, the (AS4140&V1657) steel materials can be applied to wheel - rail in the railway systems.

Contents

LIST OF TABLES

LIST OF FIGURES

NOMENCLATURE

P- Contact pressure distribution

a-the half width of contact area in x direction

b- the half width of contact area in y direction

R_1- Wheel radius

R_2 -rail lateral section curve radius

E_1-young's modules of wheel

E_2- Young's modules of rail

v_2 - Poisson's ratios rail materials

v_2 - Poisson's ratios rail materials

Θ- is the angle between the principal axes

Ψ- angle between the radius of the wheel and rail

W - is the total normal contact force

A– Circumferential area of wheel treads

α– Deceleration of the vehicle

d– Diameter of wheel

F_b – Braking force

h - Heat convection coefficient

K_v- Air speed factor

K_{air}- Conductivity of air

N_u - Nusselt number

q – Heat flux generated at the tread of wheel

R_e - Reynolds number

r_w – Radius of wheel

t_b or t – Braking time taken by the vehicle to rest

V_{air} - Air speed

v_{air} - Kinematic viscosity of air

V_i – Initial velocity of the vehicle before braking

ω – Angular velocity of the vehicle

3D – three dimension

FE – Finite element

V_s – Sliding velocity

m&n- are coefficients given by hertz

C- Carbon

MN- manganese

AL-alminuium

Si- silicon

S-sulfur

Cr-chromium

Mo-molybdenum

CHAPTER ONE

1.Introduction

Railway transportation system, as one of the notable means of commuting systems, has served for human societies and has pursued its improvements as other promoted aspects of life. In recent years, the capacity of carrying axial loads for world railways as well as their velocities has been enhanced which results in increasing the amount of strains and stresses on lines and digression of rails. By this augmentation, interactions between railway components become more considerable.

The rolling contact of a wheel on a rail is the basis of many Rail-Wheel related problems including the rail corrugation, wear, plastic deformation, rotating interaction fatigue, thermo-elastic-plastic behavior in contact, fracture, creep, and vehicle dynamics vibration. Therefore, it has attracted a lot of researchers to various railway networks. The stress distribution is an important factor at the Rail-Wheel contact interfaces, that is, two materials contacting at rolling interfaces which are extremely influenced by geometry of the contacting surfaces, material attributes, and loading and boundary conditions.

The high energy efficiency of railway transportation is made possible by the favorably low losses in the rolling contact between the hard surfaces of the wheel and rail, which meet only in a very small contact patch. However, several undesired phenomena may occur in this contact, see Fig. 1 High vertical contact forces, but also lateral and longitudinal forces, induce stresses that may cause material yielding and fatigue. Rolling contact forces combined with friction induce wear. Traction and braking may lead to wheel sliding, resulting in rail burns and wheel flats, unfavorable material phase transformations and thermal cracks. These phenomena may create irregularities and/or worn profile geometries of the wheel and rail, resulting in poor vehicle dynamics and a further increase in contact forces and in vibrations and noise. The consequence may be discomfort and disturbance for passengers and the surroundings and also increased maintenance costs for wheels and rails and other components. Severe cases can even result in derailment induced by wheel or rail fracture or by the wheel flange climbing on the rail.

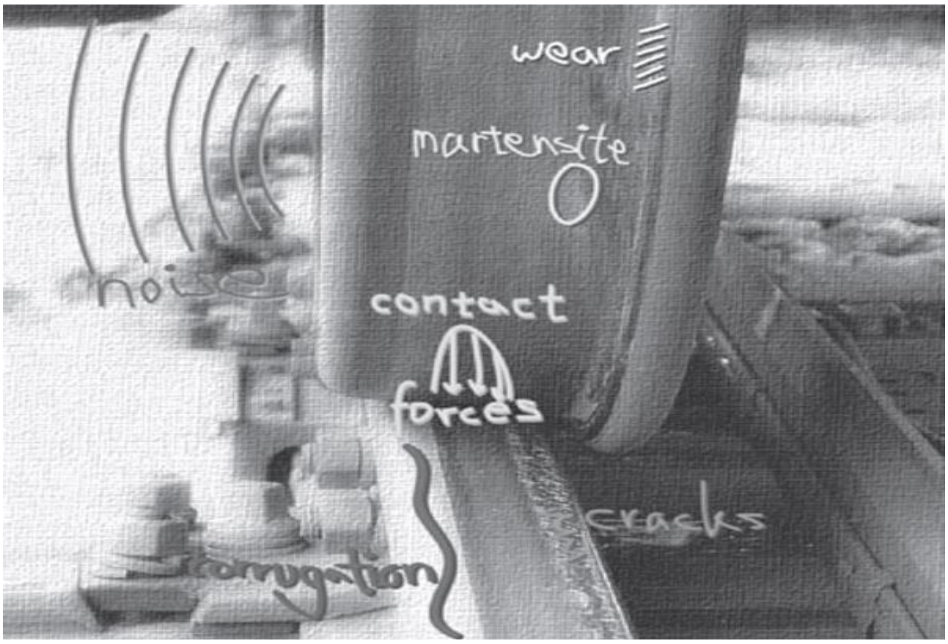

Figure 1 1.1 Several undesired phenomena may occur in the wheel–rail Interface. (Picture from Ekberg *et al*. 16)

1.1 Background

The contact condition between the wheel and rail contact, the contact zone surfaces and bulk material must be strong to resist the heavy loads and dynamic response. The contact zone must be small compared with the overall dimensions and its shape of the wheel and rail. The contact zone size and shape in the wheel and rail contact has been estimated from the Hertz theory of elliptical contact with the following assumptions: the material is linear elastic, the smooth contact surfaces, the surfaces are described by second degree and no friction between the contact surfaces. Liu [1] studied stresses due to tangential and normal loads on an elastic solid with application to some contact stress problems. Haines and Ollerton investigated contact stress distribution on elliptical contact surfaces subjected to radial and tangential forces [2]. Some useful results in the classical Hertz contact problem were presented by Sackfield and Hills [3]. The wheel–rail contact problem can be formulated as a rolling contact problem between two nonlinear profiles in the presence of friction.In the present study the behavior of nonlinear profile by considering the material properties was carried out

1.1.1 Wheel Wear

The life of railway wheels is usually limited by wear. The wheel surface is subjected to high normal and tangential contact stress. Contact forces change their magnitude and orientation when the wheel travels over the rail curves, crossings, and local surface perturbations. The contact is mostly rolling but a small amount of local sliding takes place at the interface. The amount of sliding depends on the contact patch geometry, normal force, lateral force, and friction coefficient. The removal of material from the surface by wear is a function of the sliding and contact stresses [4]. Two main manifestations of wear typically occur on railway wheels: a change in the transversal profile, called 'regular wear', and the formation of periodic wear patterns in circumferential direction, called wheel out-of-roundness or 'irregular wear' [5]. Regular wear is produced by slow variations of contact forces and creepages associated with the longitudinal and lateral motion of the wheelset on the track, on straight lines and in curves.

On the other hand, irregular wear is produced by fast variations of wheel-rail contact conditions, which are produced by train-track interaction and are strongly affected by the vertical vibrations of the system. in traction and braking, wear is produced by longitudinal tractive/braking efforts and tends to concentrate on the central portion of the wheel tread, while during curve negotiation the wear process is more complicated, and it involves both longitudinal frictional forces caused by the rolling radius difference between the inner and outer wheels and transversal frictional forces caused by the yaw angle of the wheelset [6, 7]. As a consequence of this complex wheel-rail contact condition, two distinct wear regions appear on the wheel profile: one on the flange and the other the thread, see Figure. Wear rates in these two regions depend on different factors, such as the vehicle design, the service profile, the status of the contacting surfaces (including the possible presence of natural or artificial lubrication) and the mechanical properties of wheel and rail materials

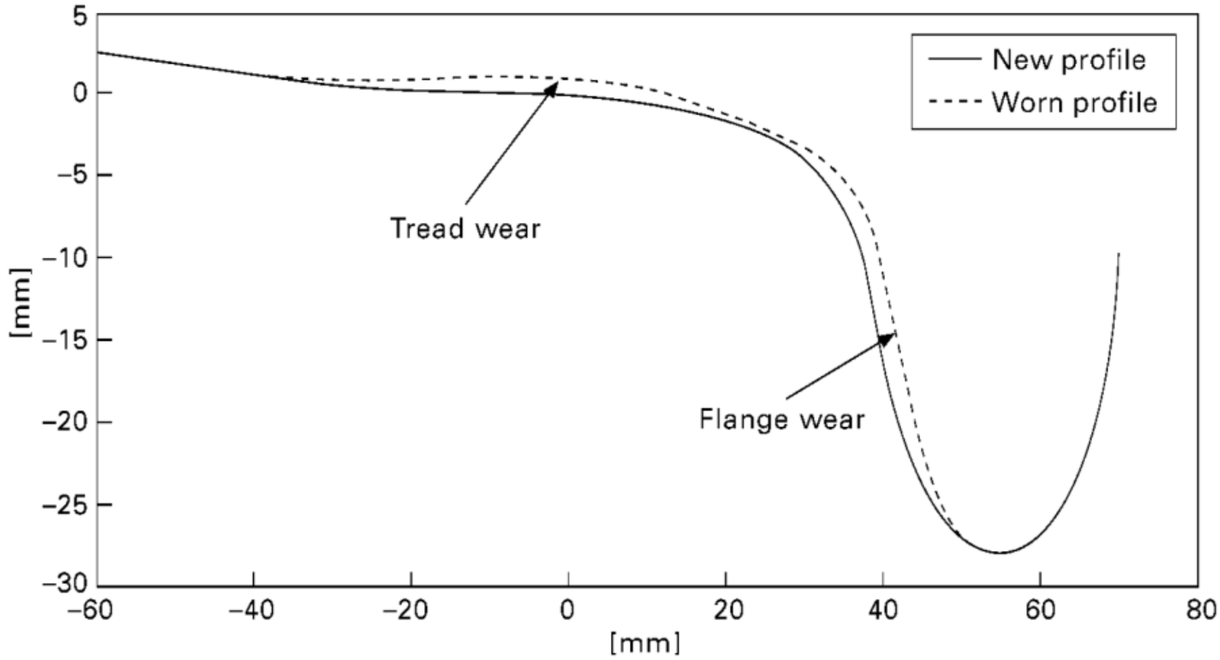

Figure 2 Wear regions on the wheel profile. [16]

1.2 Statement Of Problem

The susceptibility of railway wheel and rail to wear and rolling contact fatigue damage is influenced by the properties of the wheel and rail material .These are influenced by the steel composition, thermal and mechanical loading during operation

Damage mechanisms such as surface cracks, plastic deformation and wear can significantly reduce the service life of railway track and wheel .Fatigue and wear in wheels is often due to the forces and loading. These certainly have fundamental effects on reducing the wheel life and increasing the costs related to repairing and maintenance. Thermal load is one load type that can affect (damage) railway wheels and rail. During braking there is frictional heat produced between wheel and rail, this frictional heat is a thermal load on wheel and rail. The thermal load will produce high stress on the wheel and rail especially for a greater axle load and vehicle speed, which leads to wear. Wear on wheels can create discomfort for the transportation of goods; needs more maintenance cost, and will be a cause for more damage on the wheel. However the thermal load stress depends on the material property of the wheel; identification of better material that can resist the effects of thermal load even for higher and axle load will help to prevent wear and goods ride discomfort; reduce maintenance cost and other damages

The contact condition in terms of contact pressure and sliding velocity are found to be more important than the grade of steel [8]. Assessment of contact stresses at the wheel-rail interface thus poses every important issue in a study of rail-wheel contact phenomena. It is important to understand here that rail wheel contact pair's profile radii change with time and wear.

This has drawn much attention of many researchers to investigate the problem mainly by means of theoretical or numerical approaches for the solution of Hertz theory[9]. Hertz contact theory appeared in 1881 to solve the problem of pressure distribution between two elastic spherical bodies in contact. Later he extended it to general case of two elastic bodies in contact. Then onward sresearchers have used this theory for the analysis of the wheel-rail contact problem numerically to reach a more realistic solution. A practical and accurate formulation is still in demand [10]. The contact-pair topology influences the contact stress magnitude and shape of contact area.To speed up the process of calculation and accurate the model,.

1.3 Objective

1.3.1 General Objective

The general objective of this thesis is the stress analysis on influences of material at contact of wheel - rail by using ANSYS soft ware.

1.3.2 Specific Objectiv

- The purpose is to take one standard wheel material and pair it with another standard of rail material and run them together on ANSYS.
- Identify the best material in terms of higher stress distribution rate.
- To identify the contact pressure (stress) in the wheel–rail contact
- To determine the effect of temperature on stress distribution
- Investigating which wheel –rail material has better resistance of stress .

1.4 Scope Of The Study

These thesis describes that the influence of wheel –rail materials on thermal and static load and the stress distribution for the material wheel and rail contact, Operational parameters relate to rail and wheel geometries considering the thermal load during braking for two different types of wheel-rail material and the loads of the AA-LRT for two different types of wheel and rail materials at the same sliding speed using ANSYS software for analysis. The transient thermal and static structural analysis uses ANSYS mechanical solver and used to determine the dynamic response of a wheel structure under the action of time and determine the thermal and static stress on the wheel-rail contact finally investigated the best material of wheel and rail by comparison to similar analysis of AA-LRT

Limitation

The limitations of the researches are lack of data, and lack of enough reference books

1.5 Organization of the Research

The research is organized in five parts

Chapter one is the introductory as stated above which contains the general background, statement of problem objectives of the research, scope and limitation of the study and methodology and structure of the thesis Chapter two, a review of literature relevant to this thesis work, which has been investigated by different researchers, is given. It also briefly describes the finite element formulation of the sandwich material and finally the raised topics are summarized Chapter three shows the appropriate selection of material and the numerical calculations had be done and the simulation process that used finite element method (FEM) to analyze the wheel and rail contact modeling of the wheel rail contact by using catia Chapter four. It also contains a discussion of the results and Chapter five gives conclusion achieved from this thesis work and proposes future work in this field of study.

CHAPTER TWO:

2 LITERATURE REVIEW2.1 Introduction

This is one of the portiosof the paper that reviews the previous related works which are basic guide for the introduction of the current work. Some of them may have a direct relation with this work whereas the others may have indirect relations. But the main principles they have used and the major methodologies and approaches they precede will be selected generally and applied for the formulation of specific model and analysis. Generally there are many journals, conference papers, proceedings, design works and books related to the railway engineering, railway vehicle dynamics and particularly wheel rail dynamics, contacts, interactions etc. but to save time and to manage the paper work the review of literatures mainly considers more related works to the paper. This intensifies the deep analysis of the previous related works and selection of appropriate conditions, approaches and methodologies for the successful accomplishment of the paper

2.2 Contact Of Wheel and Rail

Contact analysis can be traced back to 1882, in which Hertz studied the elastic contact between two glass lenses. The Hertz theory is restricted to the normal frictionless contact between an elastic half–space with small deformation.

Vahid Monfared [28] presented the contact stress analysis in rolling bodies by finite element method to analyse the pressure of collection of the wheel and rail, elliptical, rectangular and circular contact surfaces are assumed for this study using classical mechanics approach. Jabbar–Ali Zakeri et al [29] studied the effect of geometrical parameters on the behavior of dynamic interaction of wheel–rail is being investigated through a parametric study. Zong et al

[30] analyzed a three–dimensionalwheel–rail contact model in the finite element framework is used for the analysisof the rail ends under wheel contact loading.

J. J. Zhu et al [31] studied anadaptive wheel–rail contact model with radial spring is developed for prediction of wheel–rail normal contact force.

Mehmet Ali Arslan and Oguz Kayabasi [32] has presented the fundamental way of handling Rail–Wheel contact problems from the FEA

Pramod Murali Mohan [33] has studied the applications of railway wheel viz., the behaviour of wheel subjected to thermal and structural loading and the combined loading. He pointed out that an excessive braking of wheel leads to thermal overloading which results in fatigue, crack propagation leading to fracture and wear

2.3 Rolling Contact Fatigue

Anderson [11] has made an effort to sort the present approaches to the RCF problem. Rolling contact fatigue (RCF) in railway wheel is caused by the rail/wheel contact and may result in initiation of surface and subsurface cracks. Fatigue performance of the wheels is a function of many factors, including service conditions, loading, material properties, environmental factors, and manufacturing processes. Rolling contact fatigue damage starts with the first mechanical operation, although it is very difficult to detect it, in fact microscopic subsurface cracks appear and propagate caused by the cyclic load applied to the railroad wheel the phenomenon of crack propagation during contact between wheel and rail has become one of the issues in railroad and a problem of intensive research in many scientific centers. Since this process is fast and uncontrolled, causes sudden break in rolling member. So, special attention is required to be paid to the life of rolling members. Fracture mechanics is widely used to predict crack growth life and several researchers have improved models to predict the stress intensity factors

Dang van et al. [12] expanded a comprehensive approach to study rolling contact fatigue (RCF) phenomenon induced by repeated rolling or rolling sliding wheel/rail contacts. They investigated cracks initiation and propagation in the rail head in a complex varying multiaxial stress regime due to Hertzian ornon-Hertzian contacts. The use of finite element method (FEM) for the fatigue life analysis and modeling crack growth is a significant step in the development of appropriate models for the accurate simulation of the cracking process in railroad wheel. Great attempt has been put into finding suitable methods to represent cracking in FEM. Some recent important findings in the fatigue life analysis and modelling crack growth have been obtained by

2.4 Heat Generations In The Wheel Rail Contact

Tanvir [13] used the Laplace transform method to determine the temperature on and under the wheel tread. He considered an elliptical pressure distribution and assumed *that the fast* moving heat source can be approximated using an instantaneous static source. He concluded that heat penetration below the surface is shallow and the thermal gradients are steep. Therefore thermal stresses should cause only surface damage

Knothe and Liebelt [14] used Laplace transforms combined with the method of Green's functions to analyze the contact temperature and temperature fields of components in relative sliding motion. To determine the temperature field in a wheel–rail contact, they reduced the three-dimensional problem, as an approximation, to a two dimensional one. Besides the temperatures on ideal smooth surfaces, derived from pressure distribution, they analyzed the effects of roughness and surface defects. Furthermore, the effect of constant and ellipsoidal loadings was investigated (Figure 3). They concluded that in the case of the examples examined, surface damages (e.g. cracks) have a higher influence on temperature rise than rough surfaces which have little impact

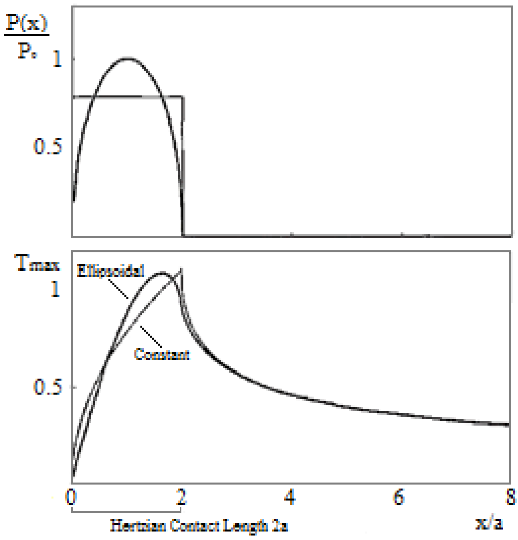

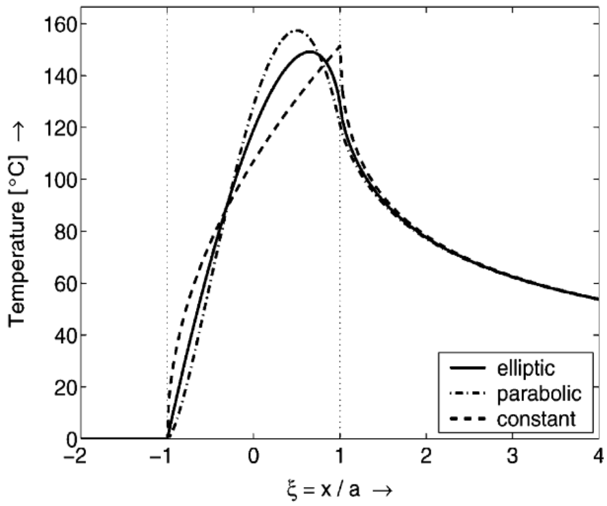

Figure 3 Normalized surface temperatures constant and ellipsoidal loads [14]

Figure 4 Temperature distribution for for different heat flow distributions [15]

Ertz and Knothe [15] used and compared semi-analytical and numerical methods to compute the maximum surface temperature in a wheel-rail contact during rolling contact with sliding friction The maximum surface temperature was determined by using the well-known Blok formula. Besides comparing different computation methods; they also compared the results obtained for various frictional heat flow rate distributions shown in Figure 4. They found that"since the average heat flow rate is equal in all cases, the maximum temperatures are almost the same". The impact of the hot wheel – cold rail contact on the temperature maximum was also examined

Gupta et al. [16] created two- and three-dimensional finite element models to investigate the temperature rise and distribution on and under a locomotive wheel tread for different combinations of creep and adhesion. The FE model they developed can be seen in Figure 15. Combining the models they could examine the maximum temperature after one hour rolling-sliding contact (for a wheel load of 147 kN). They presented a detailed diagram which shows the results of the 3D movement and a special sequentially distributed heat source model which shows the temperature distribution on the wheel tread surface during the first five revolutions (Figure 6).Furthermore, they compared the temperature distribution under the surface at the end of the first five revolutions. The results show only a little deviation between the results of the different two- and three-dimensional models. Finally, for the cases examined, they computed the heat flow rate partitioning factor as well.Figure 5 the developed two- and three-dimensional FE model used during the simulations

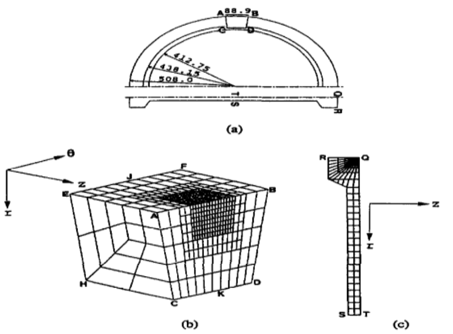

Figure 5 The developed two- and three-dimensional FE model used during the simulation [16]

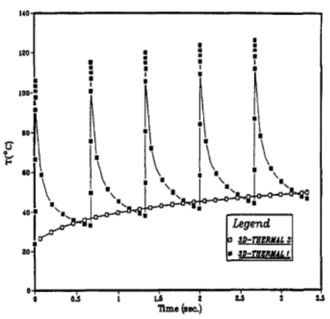

Figure 6 Temperature distribution on the first five revolation[16]

Kennedy et al. [17] used an FE model to evaluate the temperature distribution and the heat partition (the distribution of the total heat generated transferred into the wheel and the rail sights) between rail and wheel and compared the results with many analytical solutions.

They pointed out that many theoretical solutions “can produce unrealistic results under some circumstances” and hence be used to evaluate the temperature distribution and the heat partition factor between the elements in contact for high Peclet numbers

NannanZong, Manicka Dhanasekar [18] study a three-dimensional finite element method is described to investigate the effect of the discontinuity of the elastic modulus between the rail end and the insulation material in the vicinity of the gap of the IRJ. The normalized contactstress and stresses variation are presented and compared withHertzian prediction and results from Chen [18]. More importantly, the effect of various ratios of the elastic modulus between rail and the insulation material are reported

As can be seen, almost all the research focus on effects of Contact of Wheel and Rail, Rolling Contact Fatigue, Heat Generations the wheel –Rail contact, the risk on Same wheel rail material type Therefore, this paper analyze the influence of material on surface damage at wheel-rail contact by ANSYS simulation software and the result will give better Investigating which wheel –rail material has better resistance of stress (thermal &static).

CHAPTER THREE: ANALYTICAL METHODS AND CONDITION

3.1 Introduction

This portion presents the appropriate selction of the wheel and rail materials, analysis of the contact effect that occurs in the wheel rail assembly, the study being conceived on a FEA (Finite Element Analysis) calculus model.

3 .2 Materials

Wheel steel chemical analyses are shown in table below. Steels used for the manufacture of railway wheels are classified as carbon steels. Carbon steels can contain up to 1.65% manganese, 0.60% silicon and 0.60% copper with all other elements at residual levels. Railway wheel materials within the 'carbon steel' group are generally classed as medium carbon steel with some wheel steels classed as high carbon. The microstructure as manufactured is referred to as pearlite. However the lower/medium carbon steels also contain a ferrite phase which is more ductile, and adds a more resilient, impact resistant and more ductile element to the hard pearlite structure. Most alternative wheel microstructures have been investigated, but in spite of this and lack of alternatives it appears that pearlite steels offer the best performance, are inexpensive and are well understood [19]

Carbon steel classifications are illustrated in

Table 3.1 Carbon steel classifications[19]

Carbon steel Classification	Carbon %	Manganese %
low	<0.30	<1.50%
Medium	0.3-0.6	0.60-1.65
high	0.6-1.0	0.30-0.90

3.2.1 Wheel and Rail Material Selection

There is no one wheel and rail material that is right for every environment. Selecting the right wheel and rail material from the vast array of materials available can appear to be a daunting task. Careful consideration may need to be given to strength, temperature, corrosion, vibration, fatigue and many other variables. However, with some basic knowledge and understanding, a well thought out evaluation can be made [20]

3.2.2 Wheelsteel chemical analysis

Carbon: - Increasing the carbon content raises the hardness of the wheel and makes it more wear and RCF resistant. This is well demonstrated, and moving from grade B to C in the AAR standard, for example, can reduce RCF failures by 35%. The susceptibility of a wheel to RCF and shelling depends largely on the wheel hardness, so that increasing the carbon content also reduces the chances of shelling. Unfortunately, high carbon content makes the wheel much more susceptible to the thermal effects of braking and slip, because it is easier to produce brittle martensite in high carbon steel and this phase of a railway steel is more liable to thermal cracking when the wheel is braked on the tread. the resistance of the wheel to brittle fracture is reduced as the carbon content increases, and it is therefore undesirable to use a high carbon wheel in a service where tread braking or slip is at its most severe. the effect of carbon on the susceptibility of a wheel to thermal damage is complex and is difficult to predict [21]

Manganese:- has a similar effect to carbon in increasing the strength. Manganese also improves toughness, but it also makes the wheel more prone to thermal cracking. Differing from carbon, however, it does not have such a detrimental effect on the resistance to brittle fracture. Manganese also improves the depth of hardening; important in wheels throughout their service life, through many reprofilings.Manganese also increases high temperature strength [21]

Table 1 Chemical analysis of CL60 [22]

Standard	Country of origin	Grade	C	Si	Mn	P	S	CR	Cu	mo.	vn	Ni	CR+MO+NI
TB/T2 708	CHINA	CL60	0.65	0.37	0.8	0.04	0.04	0.25	0.25	N/s		0.5	0.5

Table 2 Chemical analysis of C74 [22]

Standard	Country of origin	Grade	C	Si	Mn	P	S	CR	Cu	mo.	vn	Ni	CR+MO+NI
JISE 5402	JAPAN	C74	0.77	0.4	0.9	0.04	0.04	0.3	0.3	0.08	0.05	0.3	N/S

Chemical analysis of 4140

Chromium, Molybdenum steel for applications requiring high tensile strength and toughness values, in particular in medium and large cross sections in the quenched and tempered condition. The Molybdenum additions prevent the steel from being susceptible to temper brittleness. Surface hardenable [23]

Table3 Chemical analysis of AS 4140

Standard	Country of origin	Grade	C	Si	Mn	P	S	CR	Mo.	Ni
AS	Australia	4140	0.4	0.2	0.8	0.025	0.025	1	0.2	-

3.2.4 Wheel Material Mechanical Properties

Mechanical Properties

Most wheel and rail applications are designed to support or transmit some form of externally applied load. If the strength of the wheel and rail is the only concern, there is usually no need to look beyond carbon steel. Over 90% of all wheel and rail are made of carbon steel. In general, considering the cost of raw materials.

Tensile Strength

The most widely associated mechanical property associated with standard wheel and rail is tensile Strength. Tensile strength is the maximum tension-applied load the wheel and rail can support, carry load to or coinciding with its fracture

Proof Load

The proof load represents the usable strength range for certain standard wheel and rail. By definition, the proof load is an applied tensile load that the wheel must support without permanent deformation.

Fatigue Strength

A rail subjected to repeated cyclic loads can suddenly and unexpectedly break, even if the loads are well below the strength of the material. The rail fails in fatigue. The fatigue strength is the maximum stress a rail can withstand for a specified number of repeated cycles prior to its failure

The ability to achieve the mechanical properties of each wheel grade is only achievable with a controlled chemical analysis which is not quoted in national standards, but each manufacturer has its own internal specification. This is generally a controlled amount of carbon, manganese and possibly chromium

Table 4 Mechanical properties of CL60

Standard	Country of origin	Grade	Yield strength (N/mm^2)	Ultimate tensile strength (N/mm^2)	Elongation	Hardness
TB/T2708	China	CL60	665	910 min	10	265-320

Table 5 Mechanical properties C74

Standard	Country of origin	Grade	Yield strength (N/mm^2)	Ultimate tensile strength (N/mm^2)	Elongation	Hardness
JISE5402	JAPAN	C74	670	1040-1200	9	293-363

Table 6 The mechanical properties (4140)

Standard	Country of origin	Grade	Yield strength (Mpa)	Ultimate tensile strength (MPa)	Modulus of elasticity (GPa)	Elongation	Hardness
AS	Australia	4140	925	1080-1230	210	12	311-375

Table 7 Thermal conductivity of CL60 [24]

Density (kg/m^3	7865
Thermal conductivity (W/mK)	48.6
Specific heat (J/KgK)	1685

Table 8 The thermal conductivity of C74 [21]

Density (kg/m^3)	7850
Thermal conductivity (W/mK)	50.5
Specific heat (J/KgK)	1500

Table 9 The thermal conductivity of AS 4140[25]

Density (kg/m^3	7865
Thermal conductivity (W/mK)	61
Specific heat (J/KgK)	1685

3.2.5 Rail material

The material of rail used in AA-LRT is U71Mn, rail property in accordance to EN 13674-1:2011 (E) [26]. and the chemical composition is discussed on the table 10 and 11 mechanical properties respectively. Rail material rail property in accordance to EN 13674-1:2011 (E) [27]

Table 10 chemical analysis of U71MN

Standard	County of origin	Grade	C	Si	CR	MN	P	S	AL
EN 13674	China	U71MN	0.77	0.4	0.9	0.04	0.04	0.3	0.3

Table 11 Mechanical property of U71MN

Mechanical property	Value(unit)
Young's modulus E	207GPa
Yield strength	640 MPa
Tensile strength	≥1080Mpa
Elongation	10
Density	7850 KG/m^3
Passion ratio	0.3

The material of rail U75V property in accordance to GB 2585—2007 [28]. And the chemical composition is discussed on the table 12 and mechanical properties table 13 respectively

Table 12 chemical analysis of U75V

Standard	Country of origin	Grade	C	Si	CR	MN	P	S	AL
GB 2585	China	U75V	0.71	0.51	0.9	0.04	0.03	0.03	0.3

Table 13 Mechanical properties U75V

Mechanical property	Value(unit)
Young's modulus E	207GPa
Yield strength	680MPa
Tensile strength	= 1200Mpa
Elongation	10
Density	7850 KG/m^3
Potion ratio	0.3

Chemical analysis V1657

Table 14 Chemical analysis V1657

Standard	Country of origin	Grade	C	Si	Mn	CR	mo.	v	Co
AS	Australia	V5647	0.7	0.2	0.95	0.84	0.18	0.06	-

Table 15 the mechanical properties (V1657)

Standard	Country of origin	Grade	Yield strength (Mpa)	Ultimate tensile strength (MPa)	Modulus of elasticity (GPa)	Elongation	Hardness
As	Australia	4140	1030	1393	210	12	400

3.2.6 Cost Of Wheel & Rail [27]

Table 16 cost of wheel and rail

Diameter	Place of origin	Material	Price /pieces
750mm,780mm,840mm, 920mm	Qingdao, Shanghai, Shenzhen and Other China Main Ports	ER6,ER7,ER8,ER9,R7T,R8T,R9T,CL60 C74,U71MN,U75V	US $500 - 1,000 depend on their diameter
750mm,780mm,840mm, 920mm	Hitachi Group	AS4140&V1657	US $800 - 1,100 depend on their diameter

According to the above properties

Chemical composition

AS4041 >CL60 and C74 by the composition of carbon and manganese

Where as to see the CL60 and C74 almost the same composition except small values of carbon of CL60 greater

Mechanical property

AS4041 it higher ultimate tensile strength and hardness

C74 also has higher tensile strength than CL60

AS4140 more cost

CL60 and C74 have same price

To categories wheel steels important on my thesis

To resist RCF, high tensile steels are preferred, which invariably incorporate increased carbon steels, To resist thermal damage, lower carbon steel is preferred ,To resist wear, including flange wear, an increase in carbon is preferred, and an improved quench during manufacture According to all above literature survey

I study the influences of two pair of contact materials C74 &U75V and AS4140&V1657 to compare with the AALRT wheel and rail CL60&U71MN the study on wheel/rail wear and stresses are mainly based on hertz theory and their comparison with FE analysis.

All most FE model and wear model based on archard's wear model and material model. These models are adopted to investigate the problems of wheel /rail system under the wheel/rail frictional sliding contact. The thermal and mechanical properties are used in simulation.

3.3 Method

3.3.1 Hertz Contact Theory for The Wheel and Rail

When a wheel and a rail are brought into contact under the action of the static wheel load, the contact area and the pressure distribution are usually determined using the Hertz theory In Hertz contact theory, no plastic deformation in the contact patch is assumed, and the radii of the curvature of wheel and rail profiles in the contact patch are assumed to be constant. According to Hertz theory, the normal pressure is distributed as an ellipsoid over the elliptic contact area. The ellipsoidal normal contact pressure distribution p(x,y) is expressed by [6]

$$P(x,y) = \frac{3W}{2\pi ab}\sqrt{1-\left(\frac{x}{a}\right)^2-\left(\frac{y}{b}\right)^2} \quad \ldots\ldots\ldots\ldots\ldots\ldots 3.1$$

Here, *a* and *b* are the half width of the contact area in the longitudinal *x* and lateral *y* directions, respectively, while *W* is the total normal contact force, as shown in Fig.1. The parameters are given by

$$a = m\sqrt[3]{\frac{3\pi W(k1+k2)}{4(A+B)}} \quad \ldots\ldots\ldots\ldots\ldots\ldots 3.2$$

$$b = n\sqrt[3]{\frac{3\pi W(k1+k2)}{4(A+B)}} \quad \ldots\ldots\ldots\ldots\ldots\ldots 3.3$$

The modulus k_1 and k_2 are given by;

$$k_1 = \frac{1-v_1^{\,2}}{\pi E_1} \quad \ldots\ldots\ldots\ldots\ldots\ldots 3.4$$

$$k_2 = \frac{1-v_2^{\,2}}{\pi E_2} \quad \ldots\ldots\ldots\ldots\ldots\ldots 3.5$$

$$A+B = \frac{1}{2}\left(\frac{1}{R_1}+\frac{1}{R_1}+\frac{1}{R_2}+\frac{1}{R_2}\right) \quad \ldots\ldots\ldots\ldots\ldots\ldots 3.6$$

$$A\text{-}B=\frac{1}{2}\sqrt{(\frac{1}{R_1}-\frac{1}{R_1})^2+(\frac{1}{R_2}-\frac{1}{R_2})^2+2(\frac{1}{R_1}-\frac{1}{R_1})(\frac{1}{R_2}-\frac{1}{R_2})\ (\cos(2\psi)} \ldots 3.6$$

$$\text{Cos }(\theta)=\frac{B-A}{A+B} \ldots\ldots\ldots\ldots\ldots\ldots\ldots\ldots\ldots\ldots\ldots\ldots\ldots\ldots 3.7$$

Where $R1$ and $R2$ are the wheel nominal rolling radius and the rail lateral section curve radius, respectively. Also, E_1 and E_2 are the Young's moduli of the wheel and rail materials respectively, and v_1 and v_2 are the Poisson's ratios of the wheel and rail materials, respectively. the angle of ψ is between the radius of the wheel and rail and θ is the angle between the principal axes. The values of *m* and *n* for the angle θ are given in the table below (6)

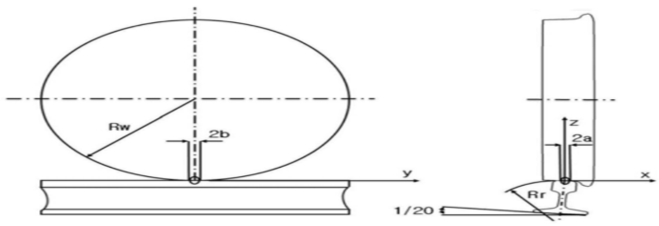

Figure 6 wheel rail contact area (6)

Table 17 Hertz coefficients

θ	m	N	θ	m	n
20	3.778	0.408	60	1.486	0.717
30	2.731	0.493	65	1.378	0.759
35	2.397	0.530	70	1.284	0.802
40	2.136	0.567	75	1.202	0.846
45	1.926	0.604	80	1.128	0.893
50	1.754	0.641	85	1.061	0.944
55	1.611	0.678	90	1.00	1.00

3.3.2 Analytical Solution for Sliding Velocity

Forces acting on the wheel during braking are shown in Figure 7. The wheel slides over rail if braking torque exceeds the adhesive torque. The wheel gets locked when Eqn. 1 is satisfied

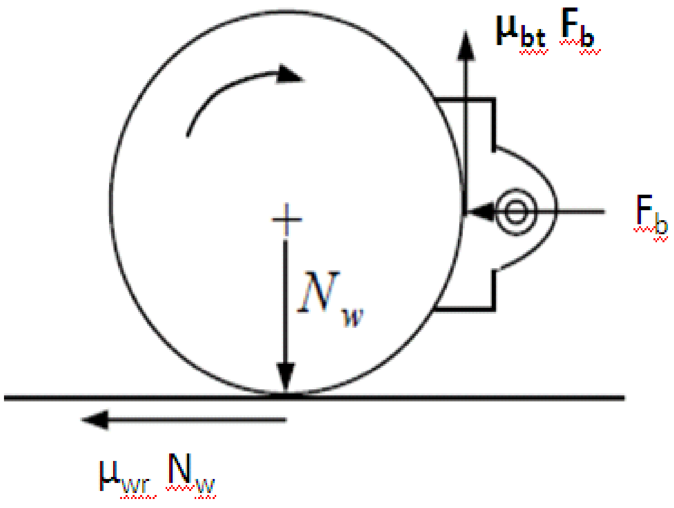

Figure 7 The assembly of wheel and tread brake

Forces on the wheel during braking

$F_b\ \mu_{bt}\ R_b > \mu_w \mu_{wr}$ R………………………………….3.8

For calculation of sliding velocity, the following assumptions are made:

· Wheels roll at the centerline

· Track irregularities are negligible

· Braking force and coefficient of friction between brake disc and brake pad do not change during sliding

Angular deceleration of wheel-set depends on the balance of braking and wheel rail adhesion

$\alpha = \frac{F_b\ \mu_{bt}\ R_b - \mu_w \mu_{wr}\ R}{I}$ …………………………..3.9

Once the angular deceleration of the wheel-set is known, vehicle deceleration is calculated using

$a_x = \frac{F_{xt}}{M}$ ……………………………………………3.10

Sliding velocity is calculated using

$$V_s = V - (a_x\, t) \quad \ldots\ldots\ldots\ldots\ldots\ldots\ldots\ldots\ldots\ldots\ldots \quad 3.11$$

Where *t* is the time required to decelerate the wheel to zero velocity and is given by the relation

$$t = \frac{\omega}{\alpha} \quad \ldots\ldots\ldots\ldots\ldots\ldots\ldots\ldots\ldots\ldots\ldots\ldots 3.12$$

3.3.3 Mathematical Model for Interface Temperature Rise

To analyses the condition where velocities of wheel and rail with respect to contact patch are different, a dimensionless parameter, *L*, called "Peclet" number, which is the ratio of the surface speed to the rate of diffusion of heat, is used. Parameter *L* has to be taken into account for heat conduction problem. As given byKnothe and Ertz [9], if *L* >10, the heat conduction occurs only perpendicular to the contact plane. In this situation, heat flow in longitudinal and lateral directions can be neglected

3.3.4 Assumption

The analytical solution for interface temperature rise was based on the following assumptions:

• There was pure sliding in whole contact area

• Coefficient of friction between wheel and rail was constant.

• Contact patch dimensions were constant and not varying with slide duration and temperature.

• The effect of elastic deformation was negligible

• The kinetic energy was transformed completely into heat

According to Knothe [9] maximum temperature rise in the wheel rail interface is given by equation

$$T_{max} = \frac{1.276\varepsilon\mu V_s P_0}{\beta_w}\sqrt{\frac{\alpha}{V_s}} \quad \ldots\ldots\ldots\ldots\ldots\ldots\ldots\ldots\ldots \ 3.13$$

Average temperature rise in the wheel rail interface was calculated from above by integrating with respect to pressure variation in the elliptical contact area and is given by the relation

$$T_{max} = \frac{0.853\varepsilon\mu V_s P_0}{\beta_w}\sqrt{\frac{\alpha}{V_s}} \quad \ldots\ldots\ldots\ldots\ldots\ldots\ldots\ldots\ldots\ldots\ldots .. \; 3.14$$

Heat generated at the interface flows through the wheel and rail. Amount of heat flow is governed by the surface temperature of the wheel and rail. Amount of heat flow to the wheel and rail with respect to sliding duration is governed by the heat partitioning parameter [26], and the relation is given

$$\varepsilon(t) = \frac{t^{0.5}}{t^{0.5} + 0.863(\frac{a}{V_s})^{0.5}} \quad \ldots\ldots\ldots\ldots\ldots\ldots\ldots\ldots\ldots\ldots 3.15$$

Thus the heat flow through the wheel is

$$q_w = (1-\varepsilon)q_f \quad \ldots\ldots\ldots\ldots\ldots\ldots\ldots\ldots\ldots\ldots\ldots\ldots 3.16$$

and heat flow through the rail is

$$q_r = \varepsilon q_f \quad \ldots\ldots\ldots\ldots\ldots\ldots\ldots\ldots\ldots\ldots\ldots\ldots 3.17$$

3.4 Dimenstion

All load data are used based on AA-LRT . Vertically downward load is sum of 3% allowance, maximum axle load. The overall load is the sum of the total tram weight and carrying capacity of the vehicle. The overall load is classified to each axle of the vehicle then the axle load is classified to each wheel vehicle. Carrying capacity of vehicle has been calculated by take average of 60kg/ person and the total rate of passenger inside of the tramcar is 317.

3.4.1 Seating capacity of vehicle

Table 18 passenger load for AALRT [29]

No	Number of passengers (persons)	Seated	Standing	Total
1	Seats (AW1)	65	0	65
2	Seating capacity (AW2) (standing 6 persons/m2)	65	189	254
3	Overload capacity (AW3)(standing 8 persons/m2)	65	252	317

3.4.2 Vehicle weight

Table 19 vehicle weight of AALRT

No	Loads	Car bodyweight	Passenger weight	Total weight
1	Empty vehicle (t)	44	0	44
2	Seating capacity (t)	44	15.24	59.24
3	Overload capacity (t)	44	19.02	63.02
4	Axle load	≤11（1+3%）t		
5	Axle number	6		

The total vertical load is calculated as follows:

- Tram car weight = 44 ton
  - The load apply on each axle = 7.333 ton = 73333N
  - The load apply on each wheel = 3.667 ton = 36667 N
- Carrying Capacity = 60kg/person *317 person = 19020N
- Over all capacity = Tram car weight on each wheel + Carrying Capacity
- Maximum Axle load = 11,000 kg * 9.81 m/s

  107,910 N

- The total vertical load = maximum Axle load +3% maximum Axle load

  (107KN + 3*107KN/100)

  =111147.3N

- The load on each wheel = total vertical load / 2

  111147.3N /2

  =55573.65N

The contact between the wheel and the rail may be modeled as two mutual perpendicular cylinders of different radii loaded against one another with a force of magnitude p it is shown that . the area of contact is bounded by an ellipse whose major and minor axis is lengths are functions material properties ,loadings and radius of each cylinder member using the properties of steel and radii of curvature wheel and the rail semi axis for the elliptical contact area are computed to be

Table 20 Parameter of wheel and rail [30]

S.N	1	2
Radii of curvature (mm)	R_{1W}=330mm	$R_{2w} = \infty$
Gauge (mm)	1435	
Axle load (N)	111147.3N	
UIC Standard (Kg)	54	
Poison’s Ratio	0.3	
Young’s Modulus (GPa)	207	

$k_w = \frac{1-v_w{}^2}{\pi E_w}$ …………………………………………….. 3.9

$k_w = \frac{1-0.3^2}{\pi*207*10^9\ m^2/N} = \underline{1.399*10^{-12}\ m^2/N}$

$k_r = \frac{1-v_r{}^2}{\pi E_r}$ ……………………………………………… 3.9.1

$k_r = \frac{1-0.3^2}{\pi*207*10^9\ m^2/N} = \underline{1.399*10^{-12}\ m^2/N}$

A+B = $\frac{1}{2}(\frac{1}{R_{1w}} + \frac{1}{R_{12w}} + \frac{1}{R_{2r}} + \frac{1}{R_{2r}})$……………………3.9.2

A+B = $\frac{1}{2}(\frac{1}{330mm} + \frac{1}{\infty} + \frac{1}{\infty} + \frac{1}{300})$

A+B = $\underline{3.18 *10^{-3}}$

A-B $= \frac{1}{2}\sqrt{(\frac{1}{R_{1w}} - \frac{1}{R_{2w}})^2 + (\frac{1}{R_{1r}} - \frac{1}{R_{2r}})^2 + 2\left(\frac{1}{R_{1w}} - \frac{1}{R_{2w}}\right)(\frac{1}{R_{2r}} - \frac{1}{R_{1r}})\ \cos(2\psi)}$

A- B$= \frac{1}{2}\sqrt{(\frac{1}{330} - \frac{1}{\infty})^2 + (\frac{1}{\infty} - \frac{1}{300})^2 + 2\left(\frac{1}{330} - \frac{1}{\infty}\right)(\frac{1}{\infty} - \frac{1}{300})\ \cos(2\psi)}$

For a straight segment the curvature of the rail is zero $\psi = 0^0$

A- B = $\underline{1.515*10^{-4}}$

Cos (θ)= $\frac{B-A}{A+B}$

Cos (θ)= $\frac{B-A}{A+B} = \frac{1.515*10^{-4}}{3.18*10^{-3}}$

θ = cos−1($\frac{1.515*10^{-4}}{3.18*10^{-3}}$)

θ = 87.27

Therefore from the above analytical results the value of theta on the curved and straight rail segment is equal that is no need of separate analysis. By using the following table (the Hertz coefficient) and linear interpolation method the value of m and n for the chosen rail can be easily obtained.

Table 21 Hertz coefficients (6)

θ	m	N	θ	m	n
20	3.778	0.408	60	1.486	0.717
30	2.731	0.493	65	1.378	0.759
35	2.397	0.530	70	1.284	0.802
40	2.136	0.567	75	1.202	0.846
45	1.926	0.604	80	1.128	0.893
50	1.754	0.641	85	1.061	0.944
55	1.611	0.678	90	1.00	1.00

θ_1 =85, m_1 =1.061, n_1 =0.944, θ_2 = 90, m_2 =1 , n_2 =1

$$m = m_1 + \frac{m_2 - m_1}{\theta_2 - \theta_1} * (\theta - \theta_1)$$

$$m = 1.061 + \frac{1 - 1.061}{90 - 85} * (87.27 - 85)$$

m=<u>1.033306</u>

$$n = n_1 + \frac{n_2 - n_1}{\theta_2 - \theta_1} * (\theta - \theta_1)$$

$$n = 0.944 + \frac{1 - 0.944}{90 - 85} (87.27 - 85)$$

n= 0.<u>969424</u>

$$a = m \sqrt[3]{\frac{3\pi W (k1+k2)}{4(A+B)}}$$

$$a = m*(\frac{3\pi * w(k_1+k_2)}{4(A+B)})^{\frac{1}{3}}$$

$$a = 1.033306*(\frac{3\pi * 55573.65(2*1.399*10^{-12}\ m^2/N)}{4(3.18*10^{-3})})^{\frac{1}{3}}$$

a=<u>0.05022m</u>

$$b = n \sqrt[3]{\frac{3\pi W (k1+k2)}{4(A+B)}}$$

$$b = n*(\frac{3\pi * w(k_1+k_2)}{4(A+B)})^{\frac{1}{3}}$$

$$b = 0.969*(\frac{3\pi * 55573.65(2*1.399*10^{-12}\ m^2/N)}{4(3.18*10^{-3})})^{\frac{1}{3}}$$

b= <u>0.04713</u>

By using the values of a and b, the Hertz stress (contact pressure) will be for Cl60&U71MN

$$P = \frac{3F_n}{2\pi ab}$$

$$P = \frac{3*55573.65}{2\pi * 0.00633 * 0.00594}$$

P = <u>705.7MPa</u>

For the contact of material AS 4140 &V1657

$$a_1 = m*(\frac{3\pi * w(k_1+k_2)}{4(A+B)})^{\frac{1}{3}}$$

$$a_1 = 1.033306*(\frac{3\pi * 55470.65(2*1.379*10^{-12}}{4(3.18*10^{-3}})^{\frac{1}{3}}$$

a_1 = 0.005

$b_1 = n*(\frac{3\pi*w(k_1+k_2)}{4(A+B)})^{\frac{1}{3}}$

$b_1 = 0.969*(\frac{3\pi*55470.65(2*1.379*10^{-12}}{4*3.18*10^{-8}})^{\frac{1}{3}}$

$b_1 = 0.0046$

$p_1 = \frac{3F_n}{2\pi ab}$

$$\frac{3*55573.65}{2\pi*0.005*0.0046}$$

$p_1 = 115$ Mpa

3.10 Tread Braking

Tread braking has been the most widely used mode of brake since the railway appeared in the world It uses block-shaped brake shoes made of cast iron or other material. The brake shoes are pressed onto the running wheel treads. The train's kinetic energy is converted into heat energy by the mechanical friction between wheel treads and brake shoes. The heat generated is then dissipated into the atmosphere and the braking force is created. The friction force K*φk induces a longitudinal static friction force B at the wheel-rail contact zone, which is applied on the wheel tread by the rail and is named the braking force If the static friction condition is kept in wheel-rail contact zone and the rotation inertia of the wheel is neglected, then we have

$$B=\Sigma(K^*\varphi k)$$

$\Sigma(K^*\varphi k)$----the sum of brake shoe friction force for one wheelset, one vehicle or one train

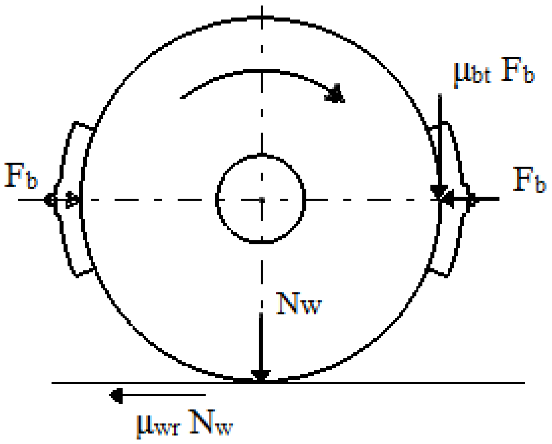

Figure 8 The assembly of wheel and tread brake

During the computations, a vehicle running at a speed of 70km/h was taken into account, with the wheels in rolling motion exposed under permanent braking. The peripheral speed of the wheels was considered to be 60 km/h*,Reference data for the presented results

Table 21 constant parameters

Semi-axis of the contact ellipse	symbol	Value	Unit
In rolling direction	a	0.00633	m
In lateral direction	b	0.00594	m
Specific heat capacity [9]	c	450	J/kgK
Normal force (wheel load)	N	55.5	KN
Maximum Hertzian pressure	P	704	MPa
Wheel radius	r	0.33	m
Vehicle speed (27)	v_0	70	m/s
Thermal penetration coefficient	β	13290	Ws/Km
Thermal diffusivity	k	14.2*10^{-6}	m^2/s
Thermal conductivity [9]	λ	50	W/Km

Table 22 The velocity AALRT [30]

Velocity	60km/h
Angular velocity	58.9
Mass of one wheel	20387.36
Deceleration (m/s^2)	1.5

Where *t* is the time required to decelerate the wheel to zero velocity and is given by the relation

$$t=\frac{v_i}{\alpha}$$

$$t=\frac{60\,km/h}{1.5m/s^2}$$

$$t=\frac{16.66\,m/s}{1.5m/s^2}$$

t = 11.1 s

The thermal energy generated by intial velocity

$$Q_{gen} = \text{K.E} = \frac{1}{2} * M * V_s^{\ 2}$$

Q_{gen} = 0.5 *20387.35*(16.6 m⁄s)2

Q_{gen} = 2808969

The power generated during braking

P = (K.E)/t

P = 2808969/11

P = 255360.82 power generated

The area A of wheel should be

$A = \pi r^2$

A=π(0.33)^2

Thus the heat flux through the wheel is

$q_w = \frac{0.95 * P}{A}$

q_w = 709087.96 W/m^2

Heat generated at the interface flows through the wheel and rail. Amount of heat flow is governed by the surface temperature of the wheel and rail. Amount of heat flow to the wheel and rail with respect to rolling duration is governed by the heat partitioning parameter [11], and the relation is given

ε(t) = $\frac{t^{0.5}}{t^{0.5} + 0.863\,(\frac{a}{V_i})^{0.5}}$ With the time [1 :11]

Table 23 The heat flow with time of 11sat contact of wheel and rail

t	1	2	3	4	5	6	7	8	9	10	11
ε(t)	0.96	0.97	0.976	0.979	0.981	0.9834	0.9847	0.9856	0.9864	0.98775	0.98775

3.11 Heat Convection

Under the analysis condition for the cooling period, the railway is accelerated up to the maximum speed of 70km/hr. and then the railway speed is maintained for the certain period. This period in which the heat energy can be transferred to the ambient through convection can be calculated from the time and distance between stations. After the cooling period, the next brake application is taken before the destination station. To determine heat convection coefficient during the cooling period, the dimensionless parameters are used such Nesselt (Nu) and Reynolds *(Re)* numbers together with the air speed factor (K_v= 0.12)

Table 24 constant for the heat convection

Nesselt (Nu)	Reynolds(Re)	Air speed factor (K_v)
N_u=0.037*$R_e^{0.8}$	$R_e=\frac{v_{air}*r_W}{v_{air}}$	0.12

Heat convection

$$h=\frac{N_u*K_{air}}{r_W}$$

$$N_u=0.037*R_e^{0.8}$$

$$R_e=\frac{v_{air}*r_W}{v_{air}}$$

$$v_{air}=k_v*v_s$$

$$k_v=0.12$$

$$k_{air}=0.0241$$

$$v_{air}=12.34^{-6}\ m/s$$

v_{air} = 0.12* 2.79m/s

v_{air}=0.3348m/s

$R_e=\frac{v_{air}*r_W}{v_{air}}$

$R_e=\frac{0.3348\ m/s}{12.34*10^{-6} m/s}$

R_e =27131.2

N_u =0.037*$(27131.2)^{0.8}$

N_u = 130.3

h=$\frac{130.3*0.024}{0.33}$

h= 9.47

The input data for the transient thermal analysis in ansys

Table 25 Input data for ansyss

The heat flux (q_w)	709087.96 W/m^2
Initial temperature	25
h	9.47

3.5 Wheel and Rail Contact Modeling

Before performing any type of analysis the solid modeling of the material is mandatory using solid modeling software the 3D model of the railway wheel and rail is created using the Catia V5software package. The modeled wheel and rail used in the analysis is the same for different case. Because the wheels are different in material composition and properties, not in structural dimension

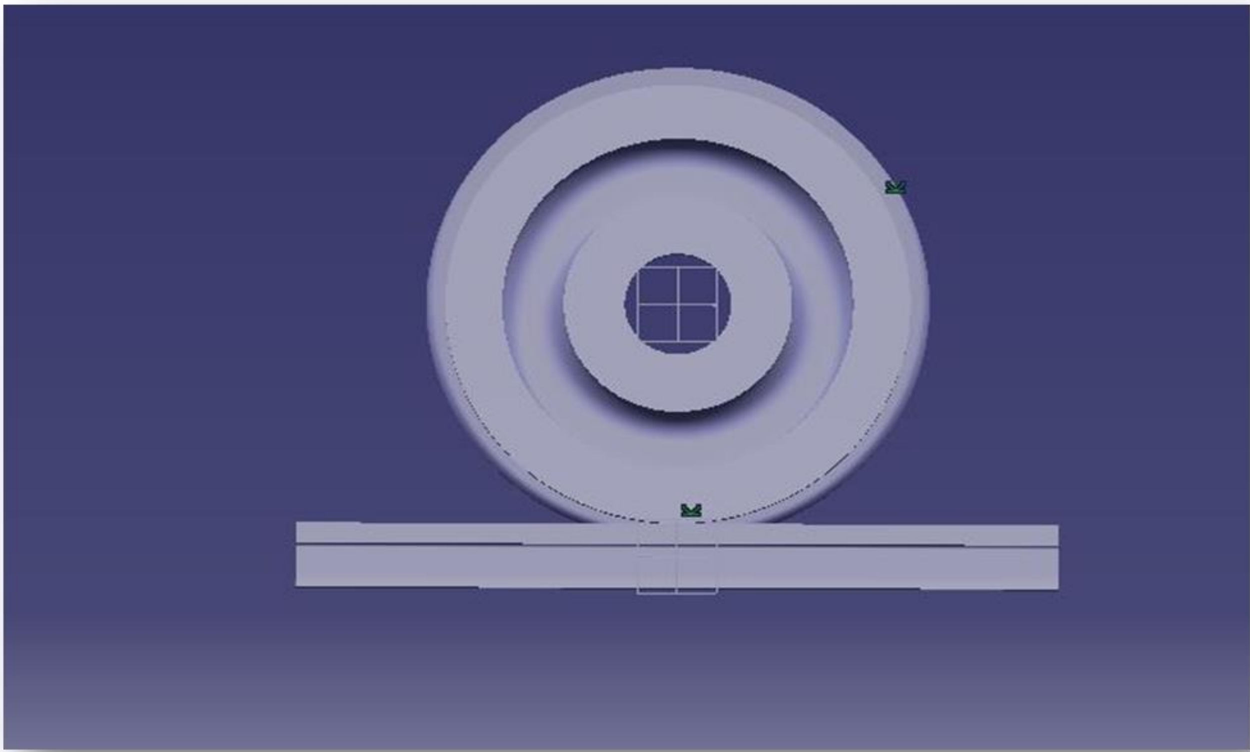

Figure 9 3D model of the railway wheel and rail

3.5.1 Finite Element Analysis

The finite element analysis (FEA) is a computing technique that is used to obtain approximate solutions to boundary value problems. It uses a numerical method called finite element method (FEM). FEA involves the computer model of a design that is loaded and analysed for specific results, such as stress, deformation, deflection, natural frequencies, mode shapes, temperature distributions, and so on. The railway track was modelled and analysed using the finite element software ANSYS 16.0

3.5.2 Meshing

Meshing is discretizing the solid object to finest parts to perform the analysis to get the precise value at each and every elements of the meshed object. This model used fine meshed method (number of element 8238 & nodes 22562)

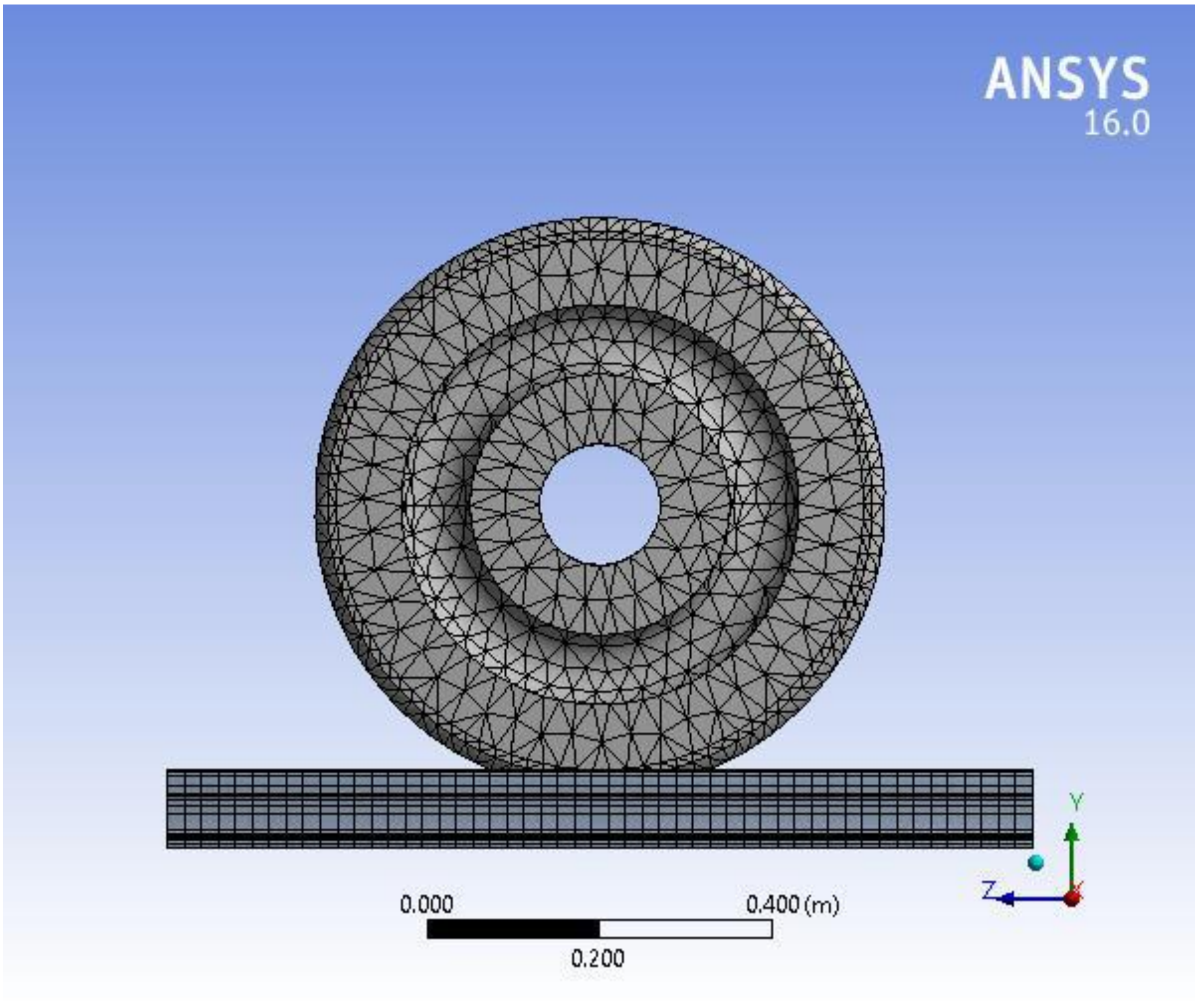

Figure 10 Meshed models of the wheel –rail contact

3.5.3 Definition Of The Boundary Condition

After completion of the finite element model and mesh, it is necessary to apply constraints and loads to the model. The analyzed railway wheel and rail contact subjected to thermal load of heat flux. As it is expressed before, the analysis is going to be done for rolling velocity the heat flux applied on railway wheel tread surface, is assumed uniformly distributed around the wheel circumference, and is equal to the rail. the applied heat flux is the same for the wheel and rail 1 and wheel and rail 2 and wheel and rail 3 since the wheels are going to be analyzed with the same thermal load and the force

The heat convection from the wheel and rail 9.47 W/m^2K

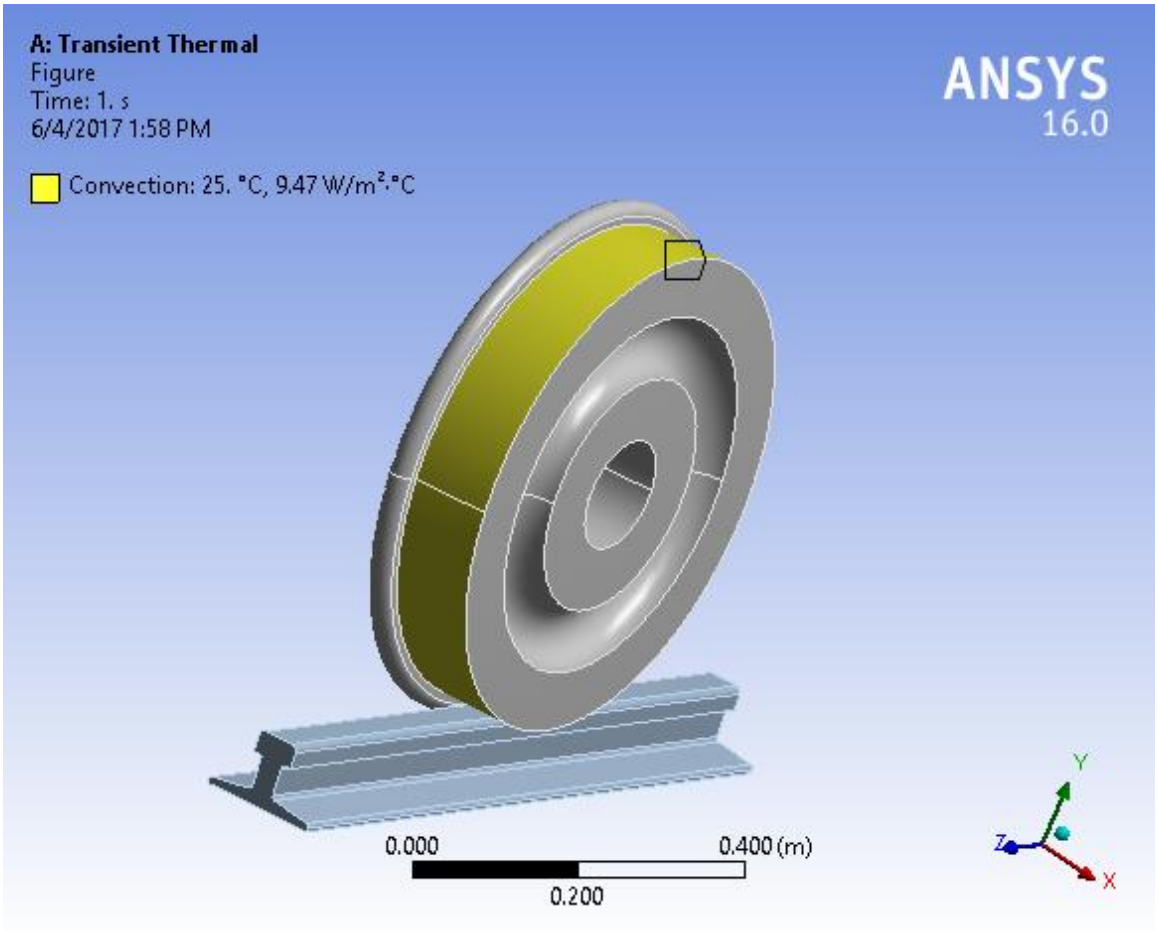

Figure 11 the heat convection from the wheel and rail at 16.6 m/s

The heat flux is applied on wheel at sliding velocity 16.6 m/s of 709087.9 W/m^2

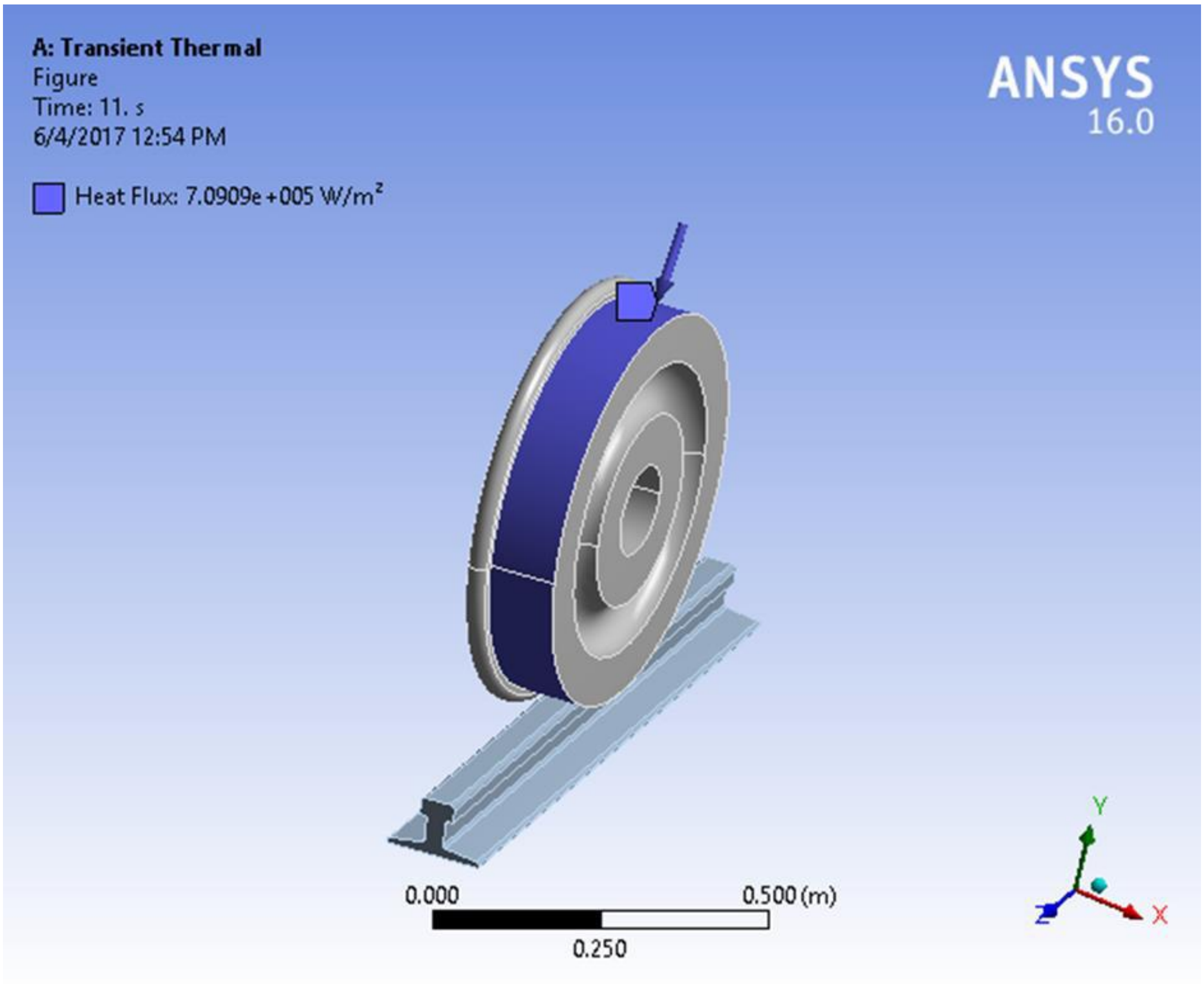

Figure 12 the heat flux applied on the wheel at 16.6 m/s sliding velocity

The force applied on the wheel 55573.65N

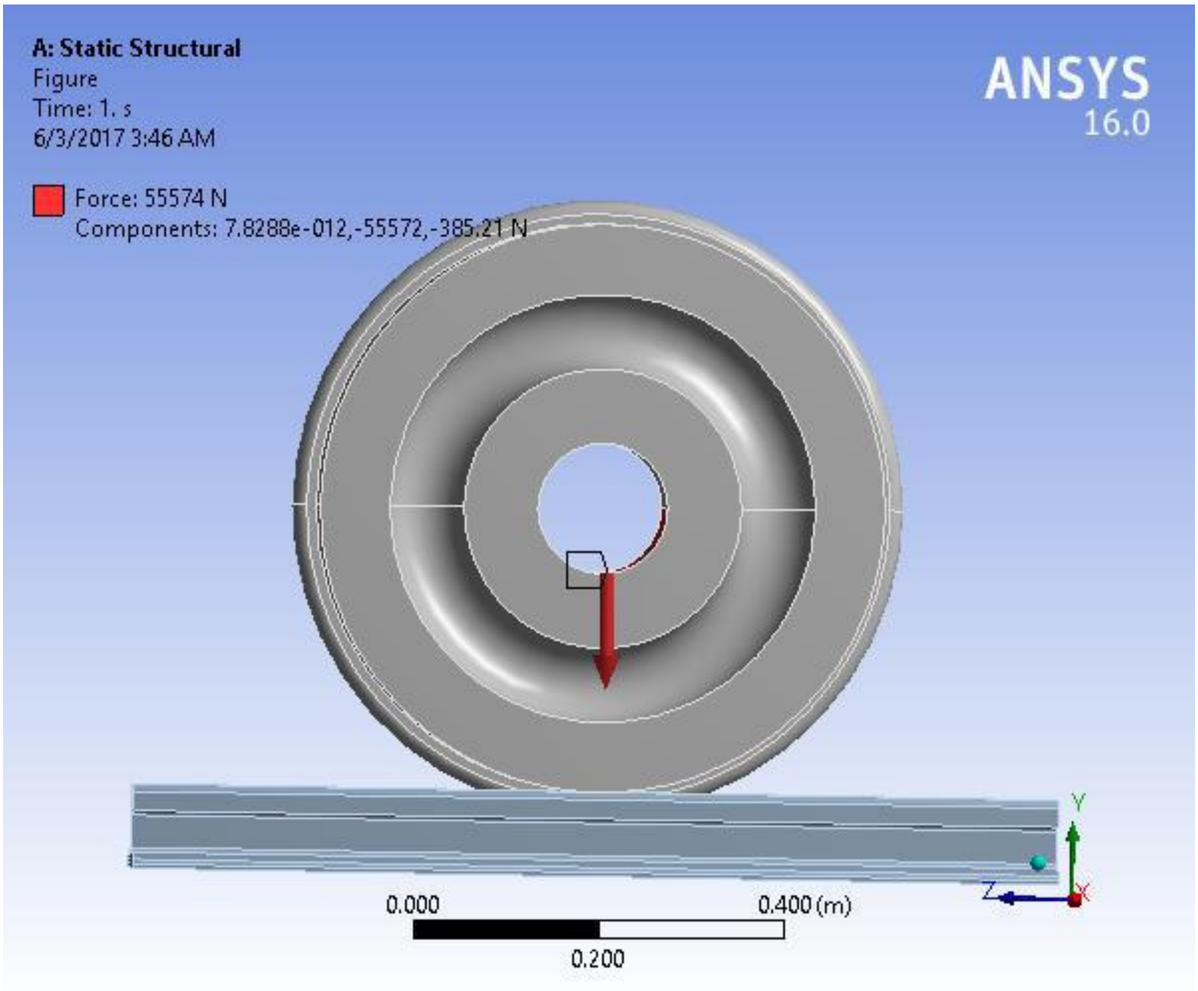

Figure 13 force applied on the wheel and rail contact 55573.6 N

CHAPTER FOUR : RESULT AND DISSCUTION

4.1 Results of thermal and static Analysis of Wheel and Rail Contact

In this part, the result of stress analysis, temperature and the contact pressure from the finite element model under different material properties will be discussed in details. Figures below show the temperature distribution on the tread of wheel AS 4140 maximum 215.98℃ and wheel C74 220.97℃ maximum and wheel CL60 223.98℃ the tread of wheel has maximum temperature that is in contact with the rail

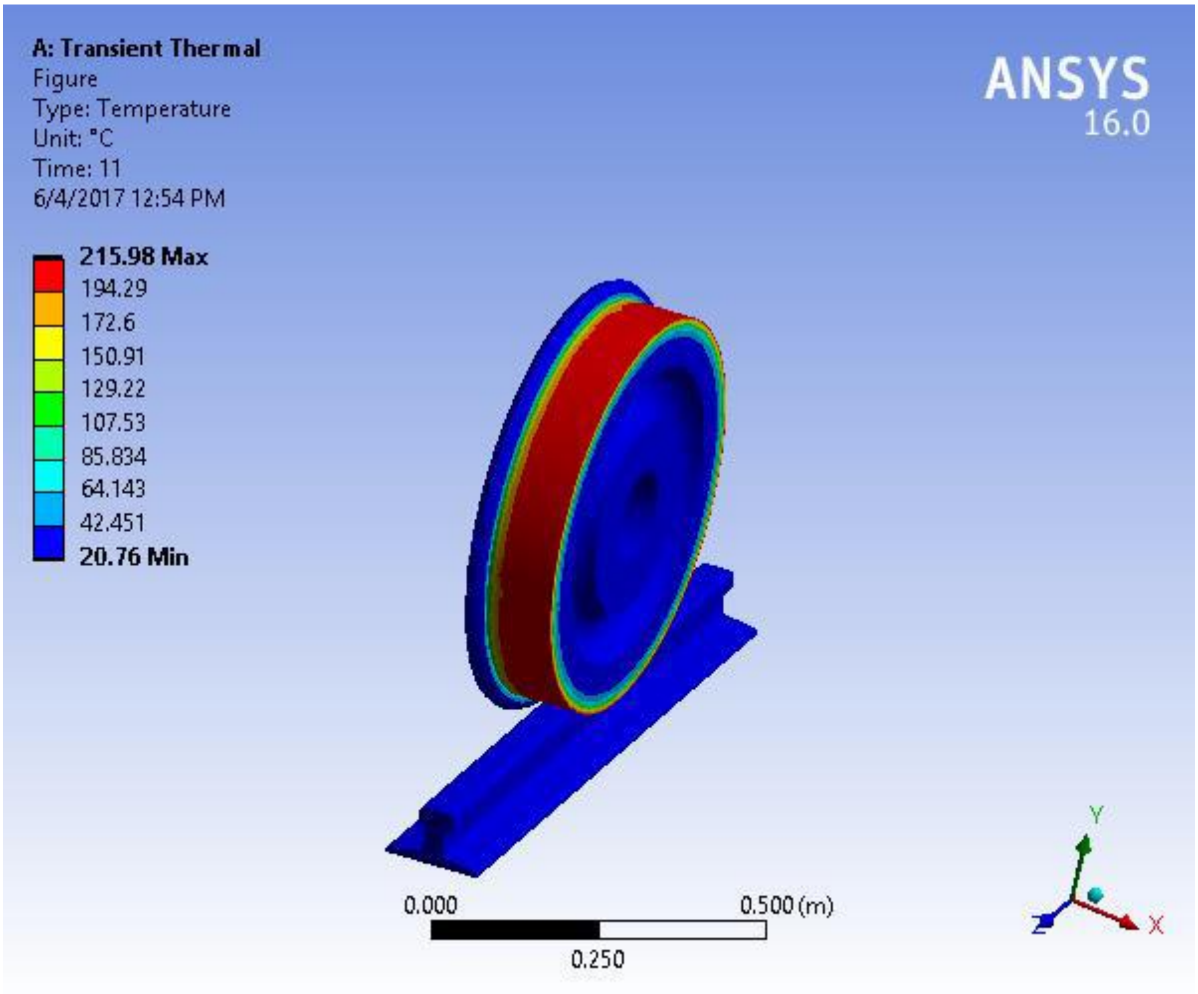

Figure14 the temperature of AS4140 wheel

The temperature of wheel of C74

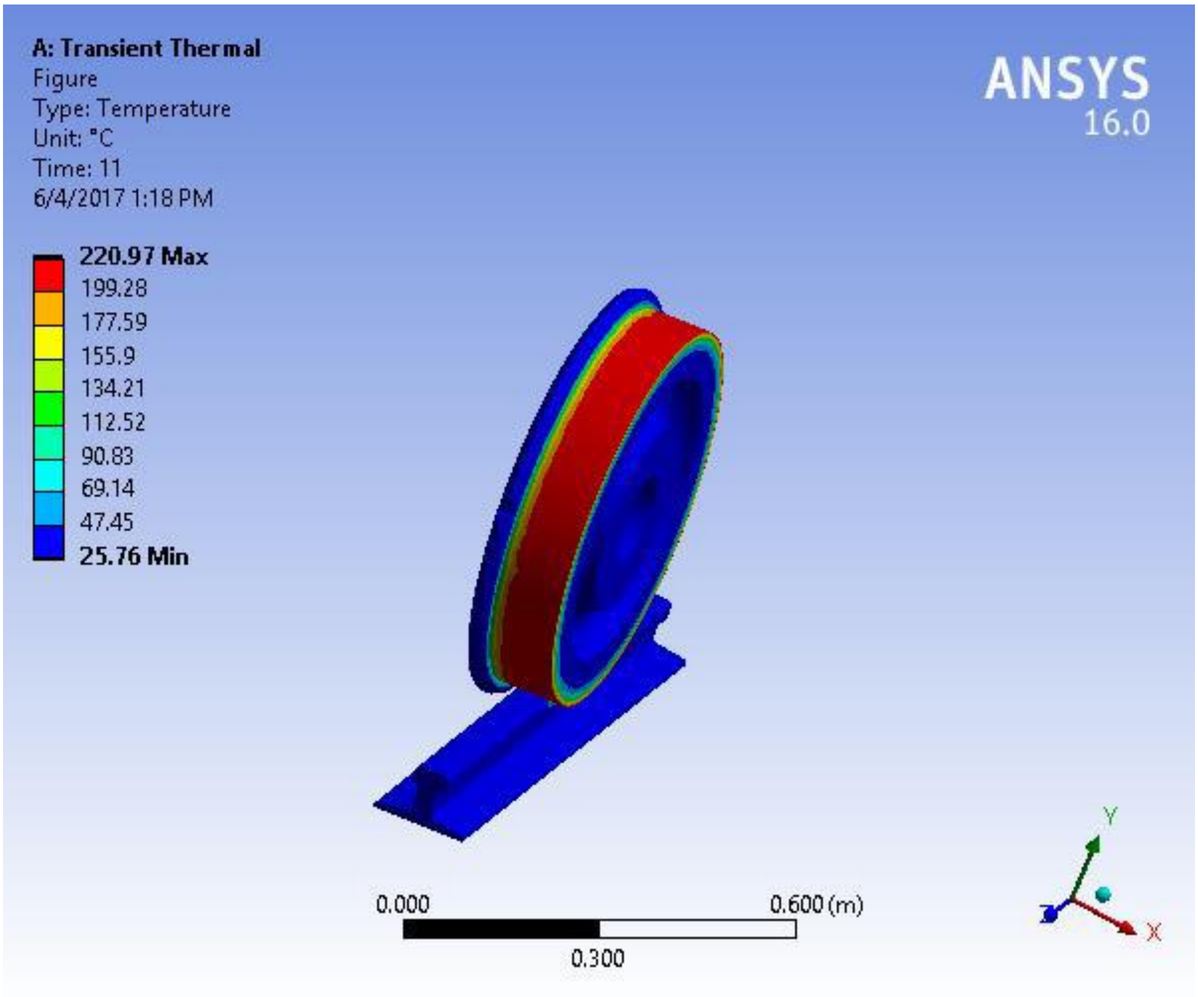

Figure 15 The temperature of wheel of C74

The temperature of wheel CL60

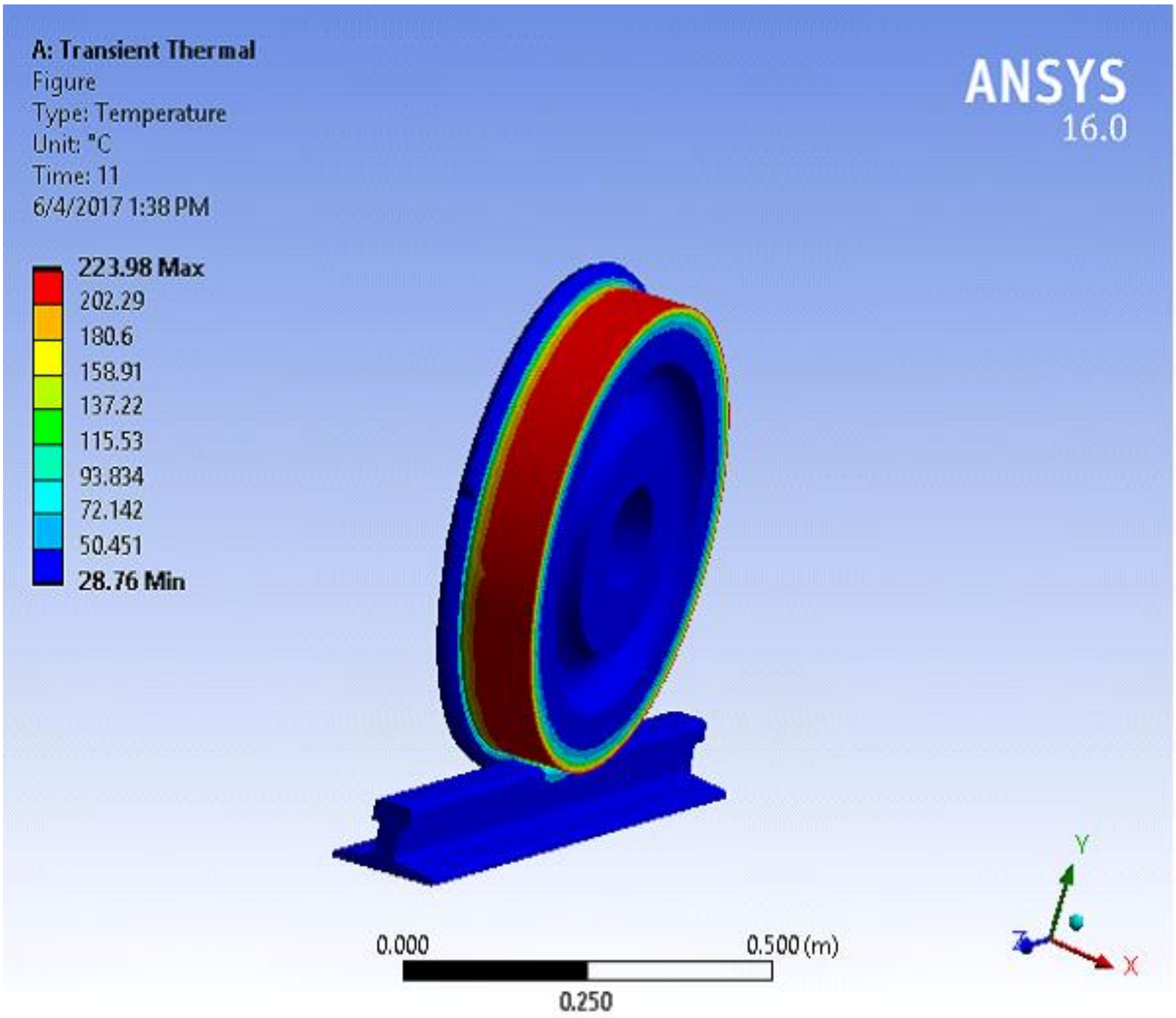

Figure 17 the temprature of wheel CL60

The follwing figure demonstrate the (Von-Mises) stress distribution on wheeland rail contact AS4140&v1657 219.9 MPa maximum and wheeland rail contact CL60&U71MN (268.2.MPa). Wheel and rail contact C74&U75V (243.8MPa) The wheel and rail part that has maximum stress is , which is in contact with at the contact of wheel and rail

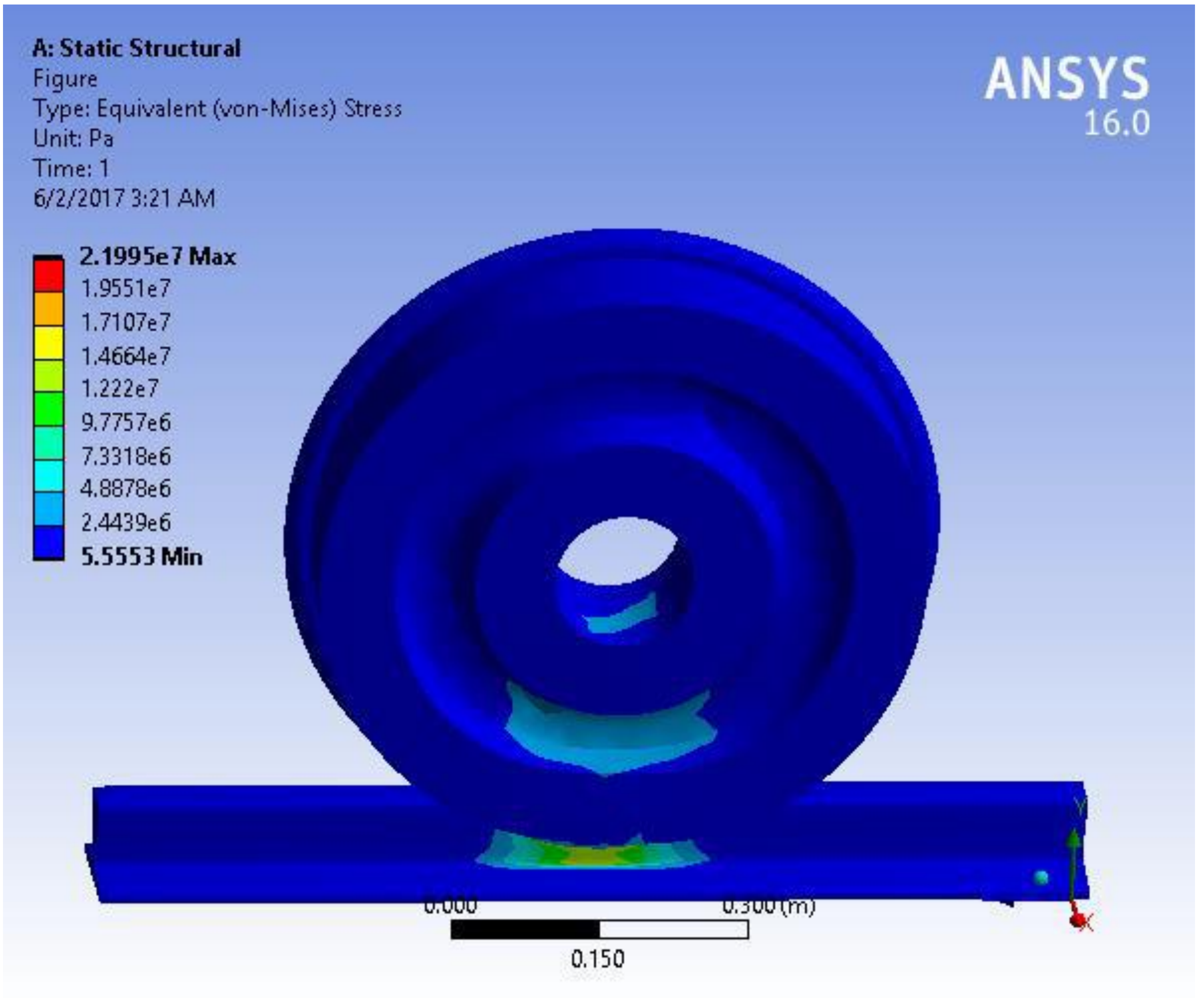

Figure 18 (Von-Mises) stress distribution on wheeland rail contact AS4140&V1657

(Von-Mises) stress distribution on wheel and rail contact CL60&U71MN

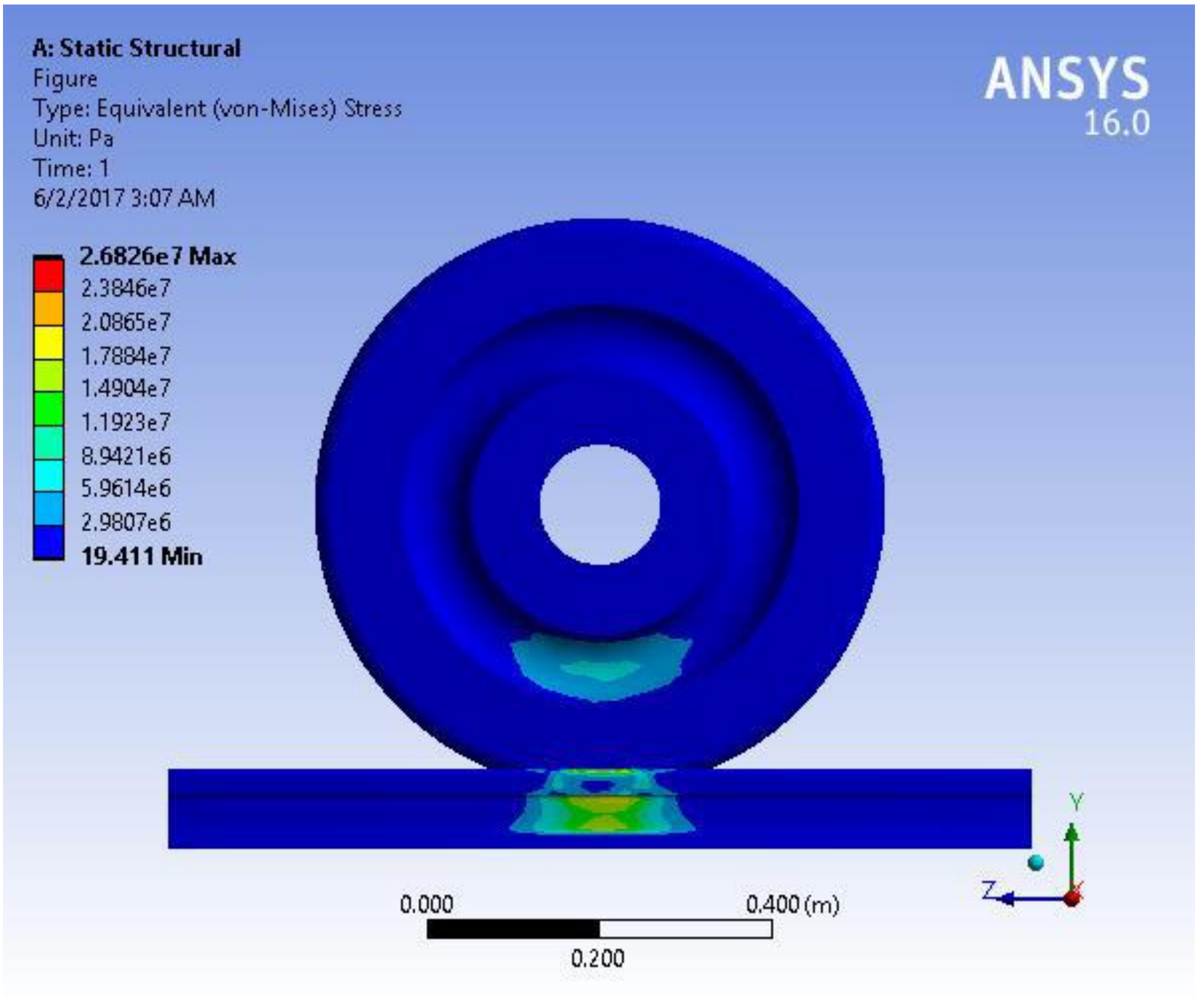

Figure 19 (Von-Mises) stress distribution on wheel and rail contact CL60&U71MN

(Von-Mises) stress distribution on wheel - rail contact C74&U75V

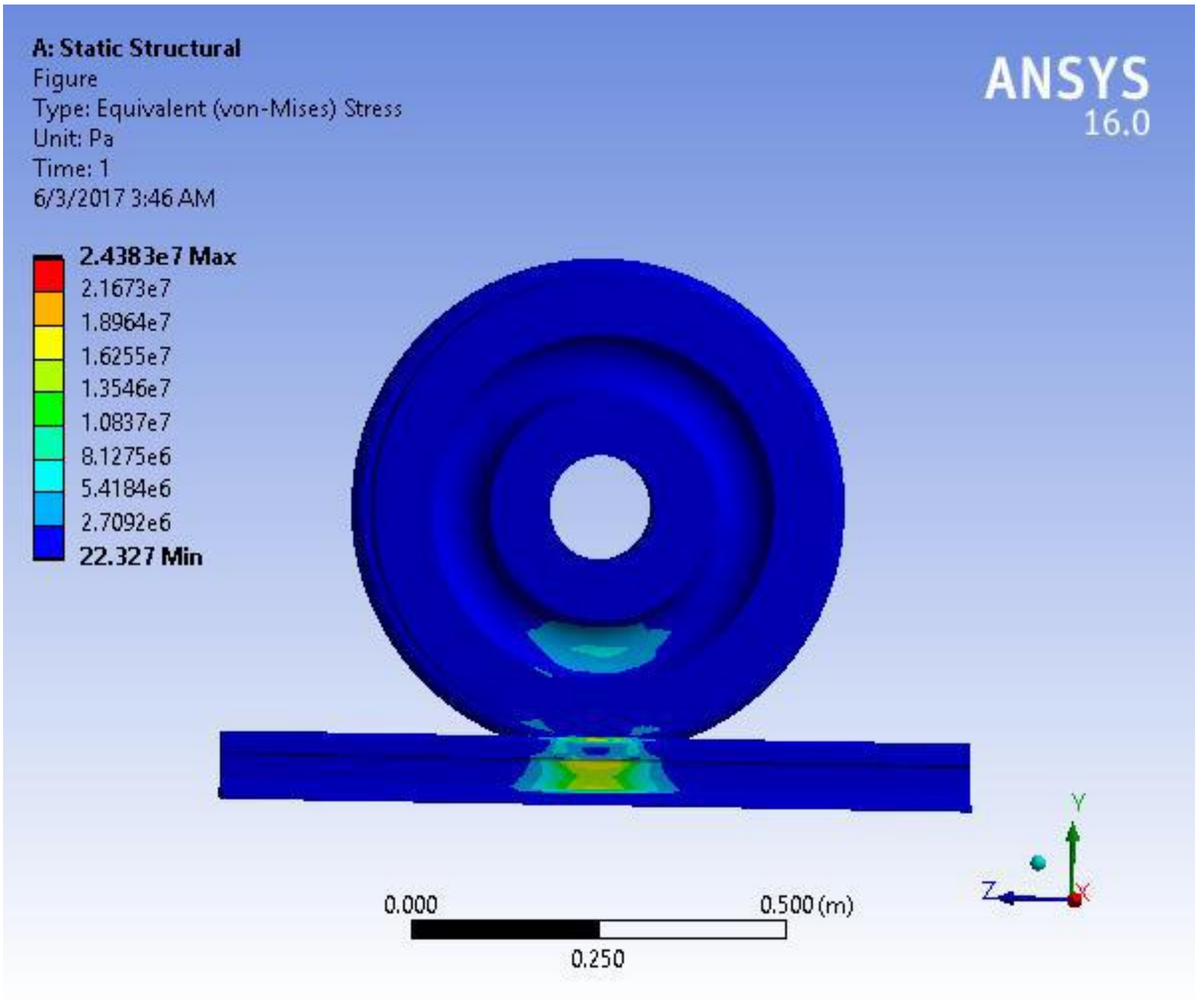

Figure 20 (Von-Mises) stress distribution on wheel and rail contact C74&U75V

The following figure demonstrate the equivalent elastic strain distribution on wheel-rail contact CL60-U71MN 0.00013955maximum and wheel - rail contact C74&U75V 0.00012937 maximum Wheel - rail contact AS4140-V1675 0.00012516 maximum the wheel and rail part that has maximum elastic strain at the contact of wheel and rail

The equivalent Elastic Strain of the wheel and rail contact of CL60 & U71MN

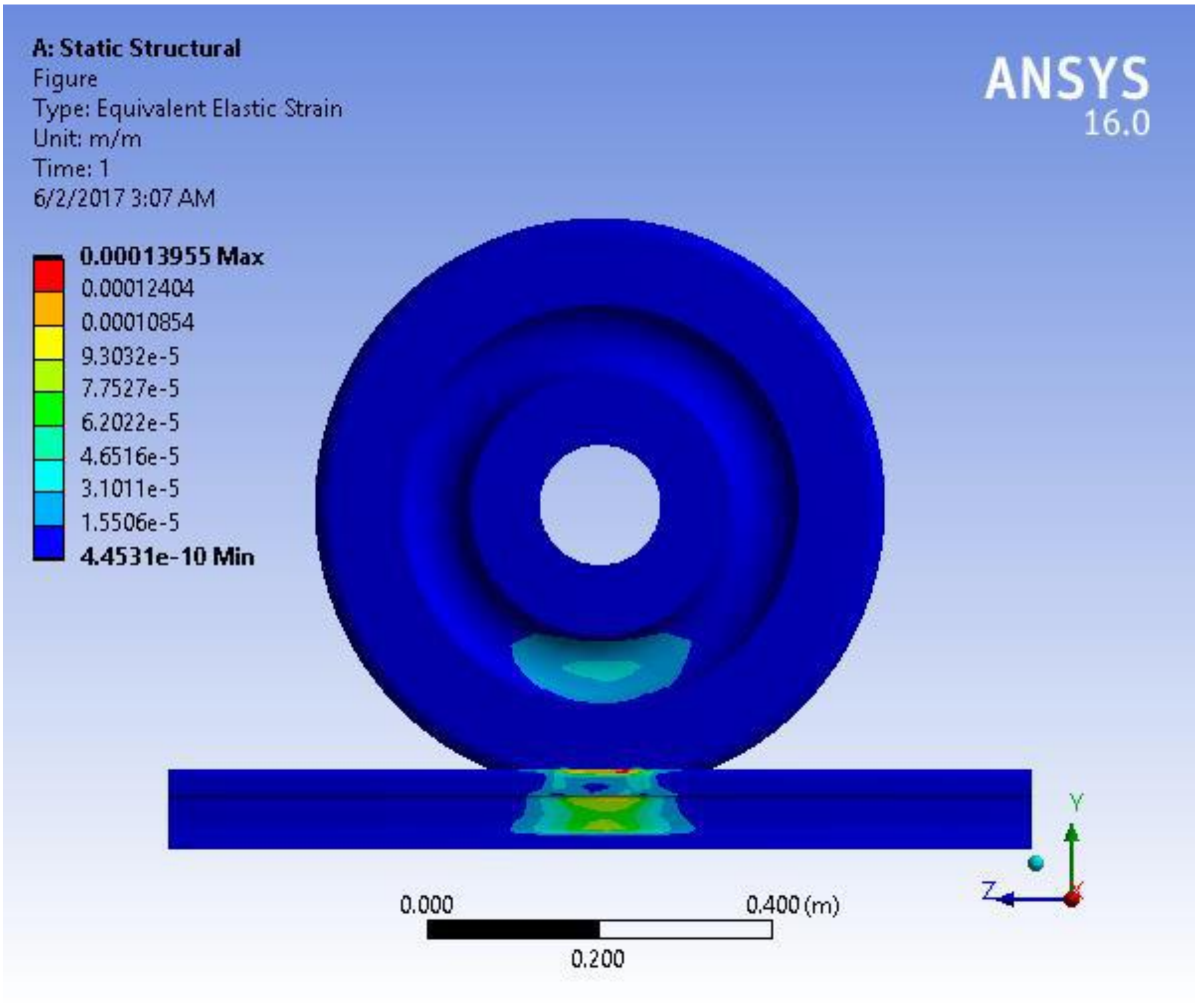

Figure 21 Equivalents Elastic Strain of the wheel and rail contact of CL60 & U71MN

The equivalent Elastic Strain of the wheel and rail contact of C74& U75V

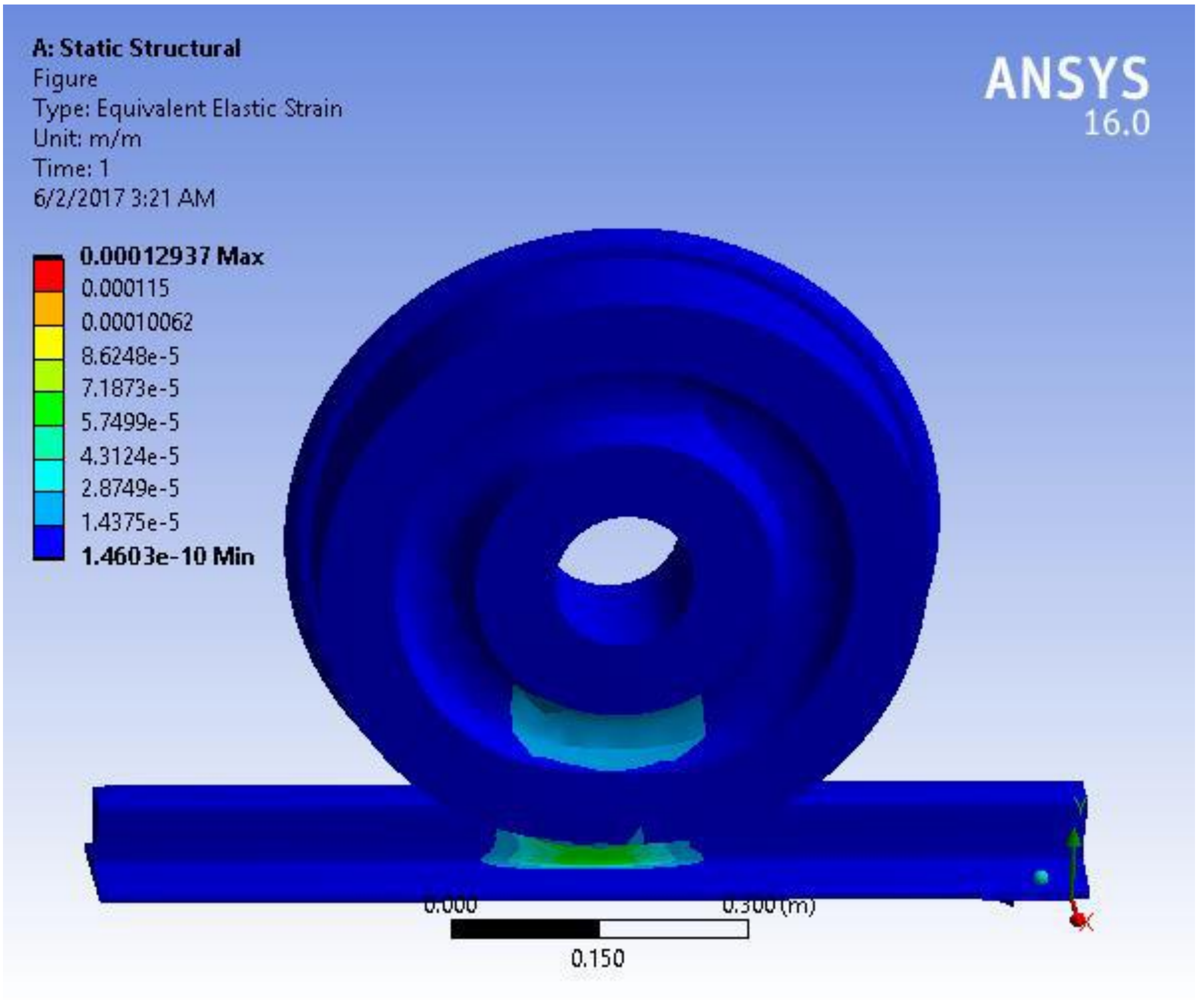

Figure 22 The equivalent Elastic Strain of the wheel and rail contact of C74& U75V

The equivalent Elastic Strain of the wheel and rail contact of AS4140& V1657

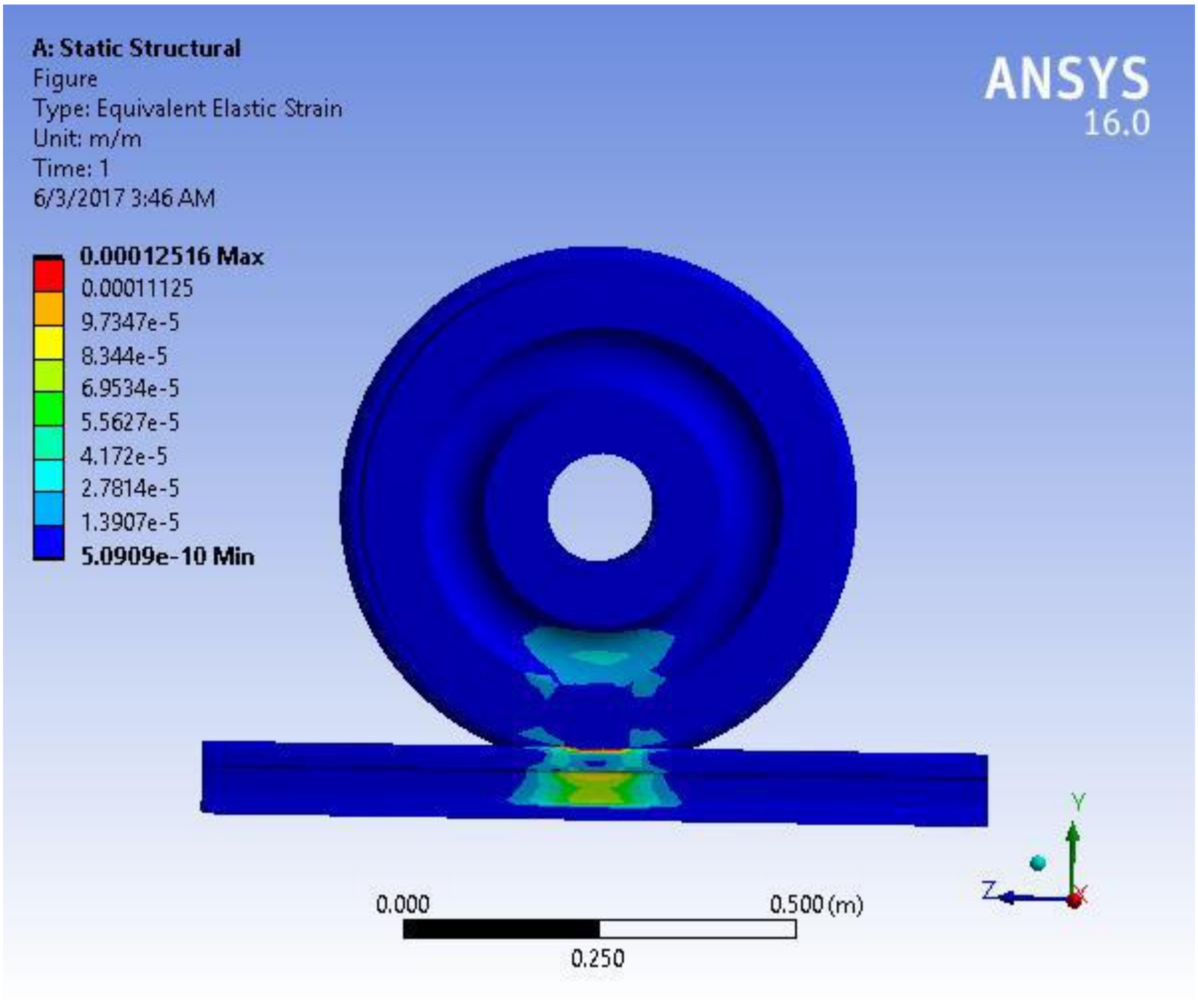

Figure 23 The equivalent Elastic Strain of the wheel and rail contact of AS4140& V1657

Demonstrate the pressure of wheel - rail on wheel and rail contact AS4140&V1657 (505.5MPa) and wheel and rail CL60&U71MN (717.6 MPa maximum). The wheel and rail contact C74&U75V (591MPa) and the maximum wheel - rail pressure distribution is on contact of wheel and rail or it the stress distbution on elliptical contacts of wheel and rail

The contact pressure between wheel and rail contact AS4140&V1657

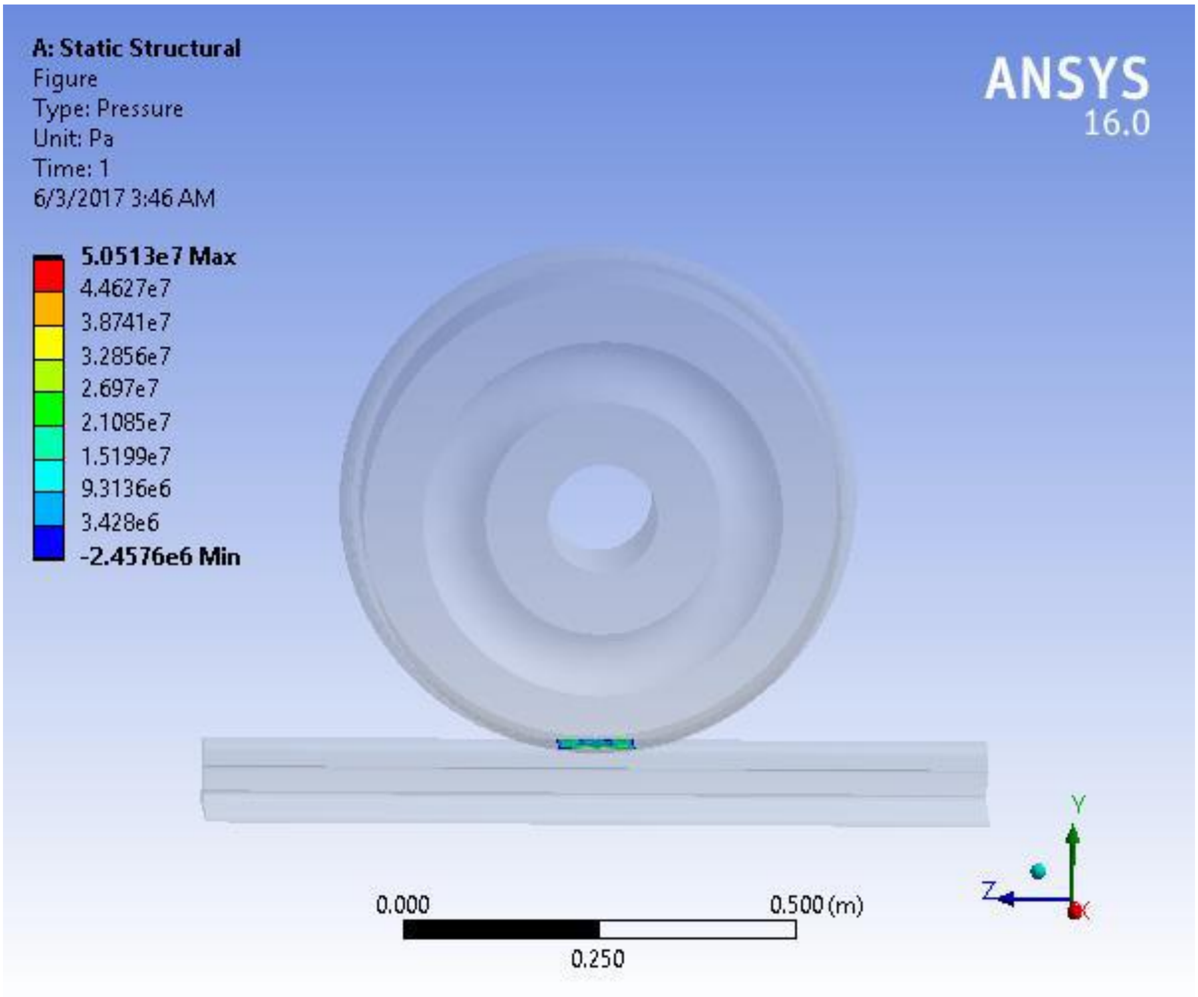

Figure 24 The contact pressure between wheel and rail contact AS4140&V1657

The contact pressure between wheel and rail contact CL60&U71MN

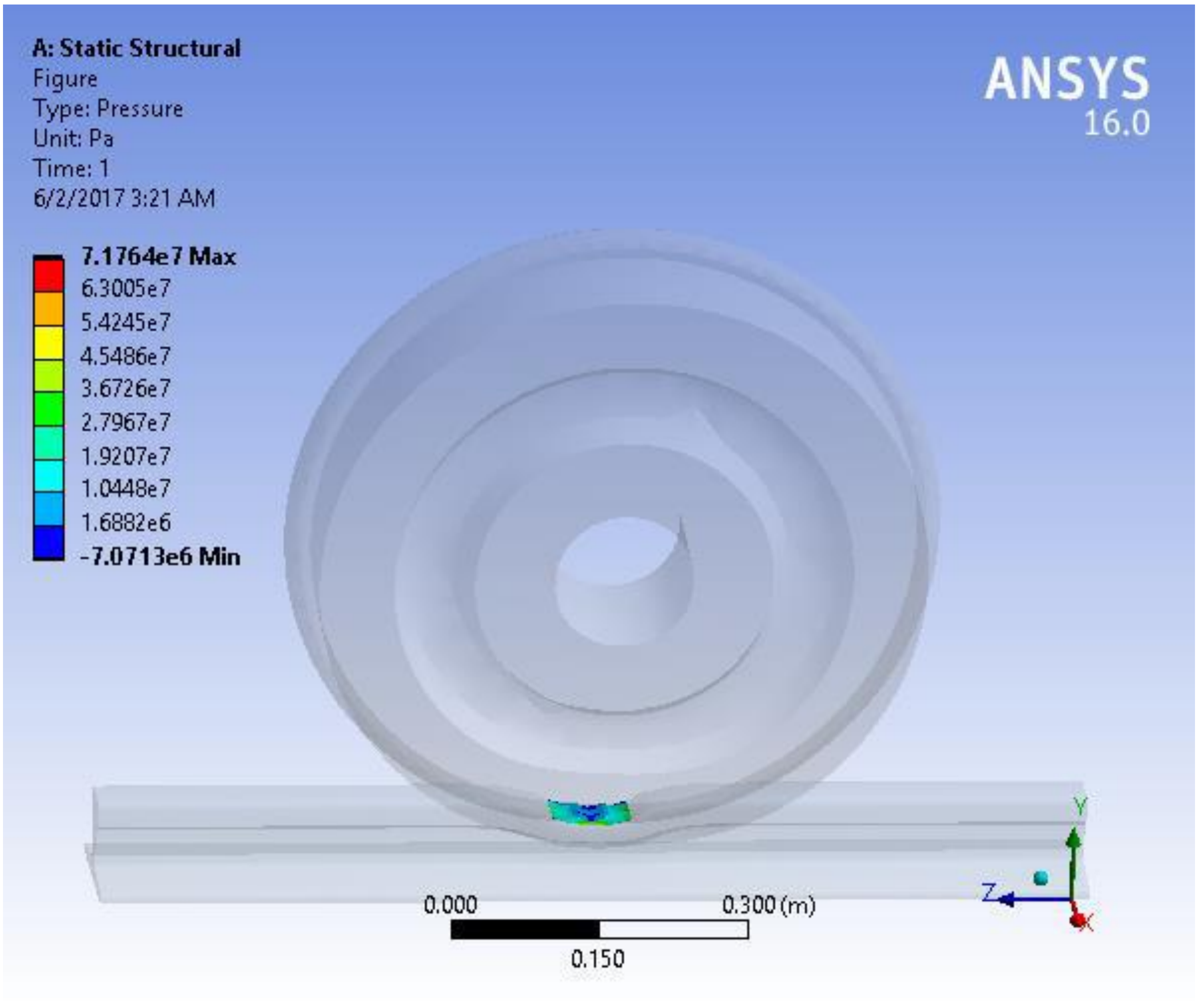

Figure 25 The contact pressure between wheel and rail contact CL60&U71MN

The contact pressure between wheel and rail contact C74 &U75V

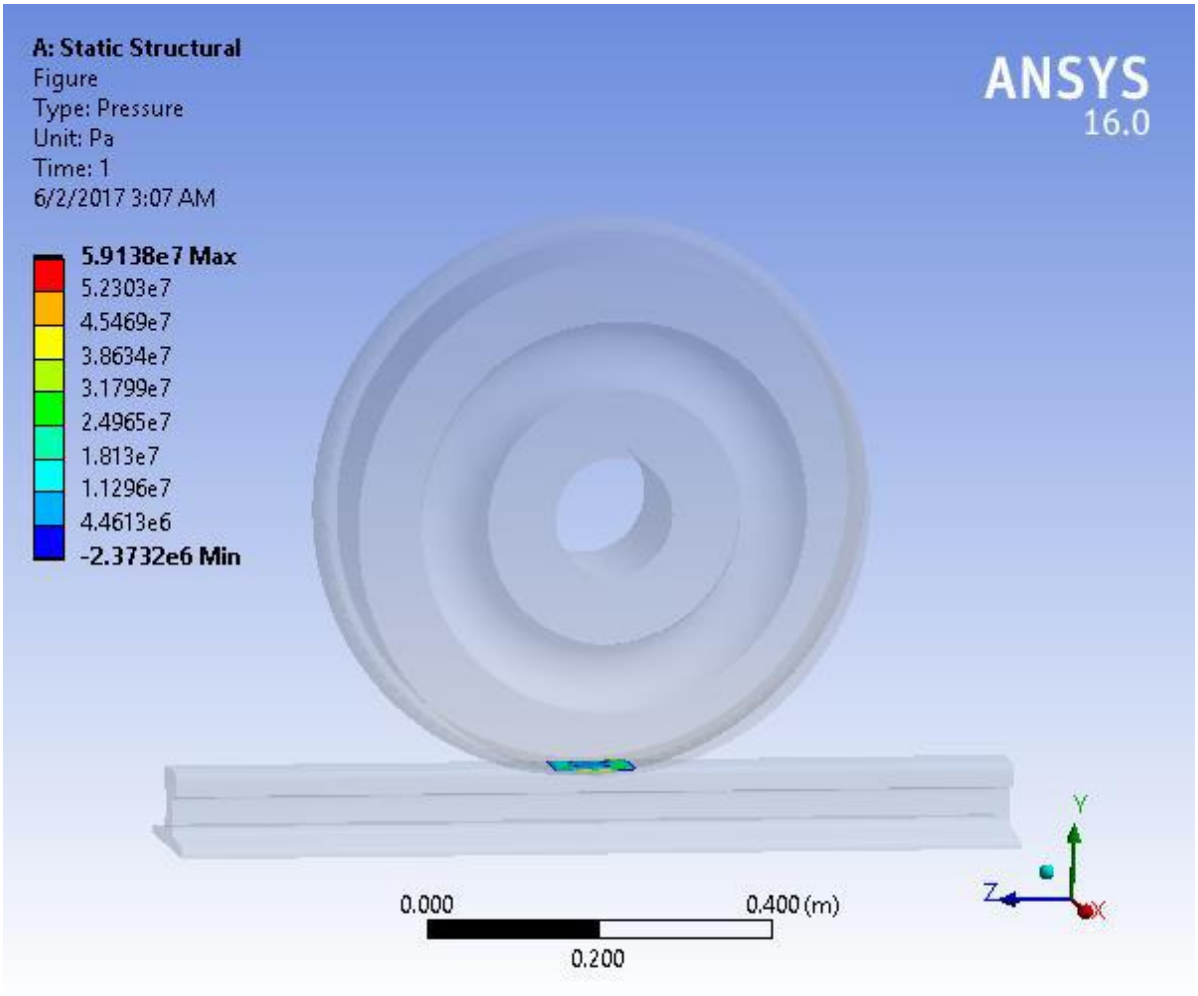

Figure 26 The contact pressure between wheel and rail contact C74 &U75V

4.2 Discussion

A finite element analysis model was developed in order to investigate all the variations of the contact temperature, (Von-Mises) stress, equivalent elastic strain, and pressure between the wheel and the rail contact at different materials was discussed in this section

Table 26 Discussion of wheel and rail contact material

Wheel and rail type Contact	Cl60&U71MN	C74&U75V	AS 4140&V1657
Intial velocity	60 m/s	60 m/s	60m/s
Temperature	215	220	223
Von-Mises Stress (MPa)	268.2	243.8	219.9
Elastic Strain (Pa)	0.00013955	0.00012937	0.00012516
Contact pressure(Mpa)	717	591	505

The temperature distributions produced for three different pair of wheel&rail materials (AS4140&V1657), (C74&U75V), (CL60&U71MN) were compared to each other. Among the investigated materials, the pair AS4140&V1657 wheel –rail showed less value this is because, the carbon content in (AS4140) is low as compare to C74 and CL60.decreasing the carbon content in the material composition improve thermal damage resistance, as well as the ductility and toughness of the material

The wheel and rail contact (Von-Mises) stress & equivalent elastic strain has been performed for different materials using the analysis software 'Ansys'. The results were obtained from the simulations

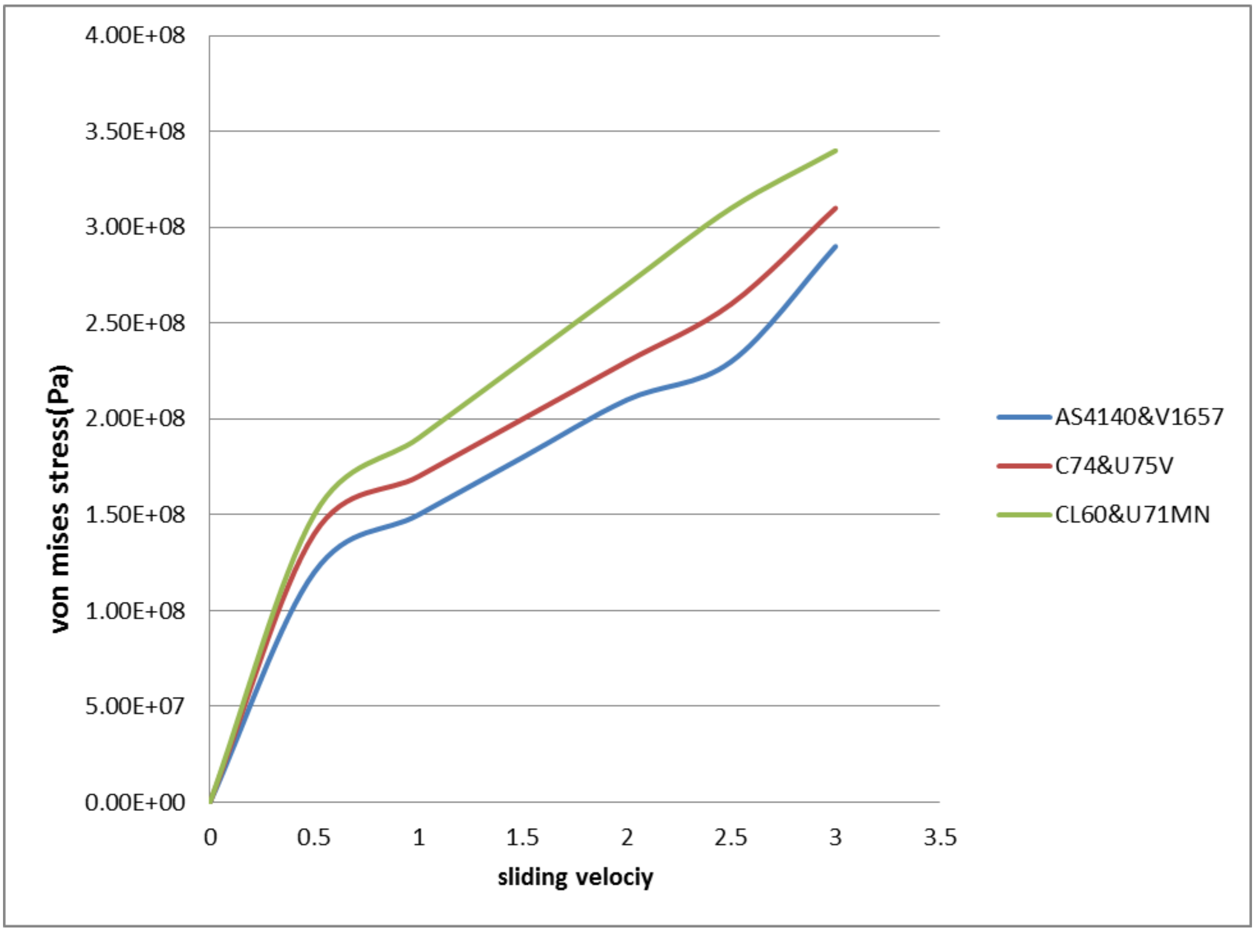

Figure 27 The graph of von mises steress versus silding velocity

In the graph above, the Von-Mises stress and sliding velocity are given for three different wheels. The result shows that the stress on the wheel-rail contact increases with increasing sliding velocity. Even though the stress increases for each wheel-rail contact the stress on CL60-U71MN is greater than the stress on wheel- rail (AS4140-V1657andC74-U75) This proves that wheel- rail (AS4140-V1657) material have better strength. This is because of the material composition difference &physical properties of material wheel- rail (AS4140-V1657) increased the hardness, strength and toughness of the material

As shown the figure above under the wheel load F=55573.6KN, the maximum contact pressure wheel-rail material (CL60-U71MN, C74-U75 andAS4140-V1657) P0 717.4Mpa, 591MPa, 505MPa varies respectively .it show that the strength of material increase the contact pressure decrease.

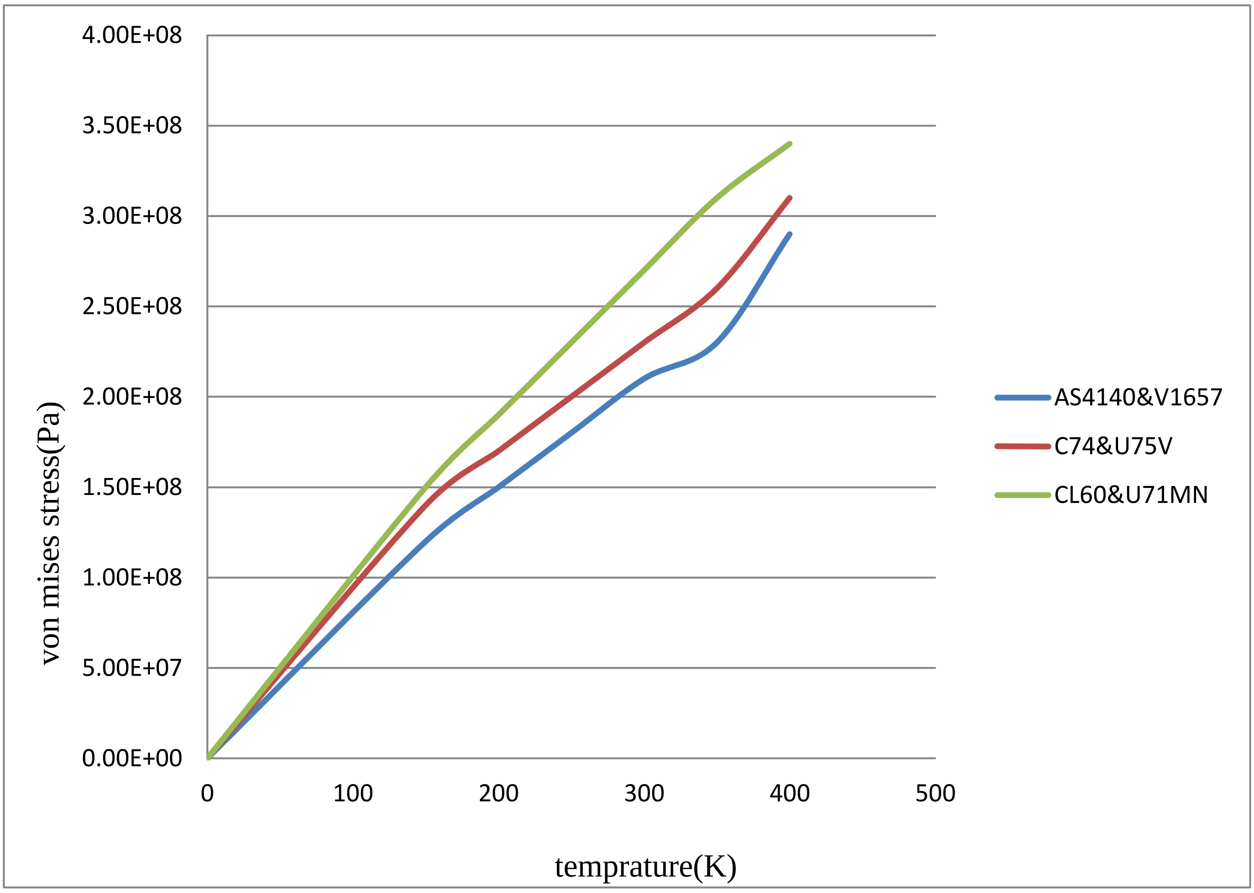

Figure 28 Temperature verses Von-Misses stress graph

In the graph above, the temperature and Von-Misses stress are given for three different wheels .and rail contact The result shows that the stress on the contact of wheel and rail increases with increasing temperature. Even if the stress increases for each wheel and rail contact the stress on CL60&U71MN and C74&U75V is greater than the stress on AS4140&.V1657 and This proves that AS4140&.V1657 material have superior strength than CL60&U71MN and C74&U75V. This is because of the material composition difference, the addition of chromium increased the hardness, strength and toughness of the material

CHAPTER FIVE : CONCLUSION, RECOMANDATION AND FUTURE WORK

5.1 Conclusion

In this thesis the wheel-rail material, for AALRT passenger trains was optimized. This was achieved by wheel rail contact models using catia & stress analysis by Ansys software. Results obtained and observations made for the stress (thermal & static) analysis of influence of different wheel - rail material property which are temperature, Von-mises stress Elastic strain and contact pressure

From the present work, several types of conclusions may be drawn as the following:-

- The performance for wheel - rail contact has been studied for different material properties.the simulation results of wheel - rail contact model shows that the maximum stress, strain are occurred in the surface of the contact. according to the results, theVon Mises stress, the strain and pressure occurs on wheel–rail contact materials (CL60-U71MN) and (C74-U75V) compare with (AS4140&V1657) under the load 55573.6 KN.
- Von Mises stress, the strain and pressure in the contact of wheel –rail (C74-U75V) lower than (CL60-U71MN) in same kind of contact.
- During braking there is heat produced between wheel and rail, this frictional heat load is applied to three wheel and which have different chemical composition and property, but same structural dimension. The wheels - rail contact are analyzed for initial velocity (60m/s). The result obtained is that AS4140 is better in resisting thermal load stresses because of its improved chemical composition and material properties than CL60&C74. when compared with cost (AS4140-V1657) greter than $60 than cost of (CL60- U71MN) and (C74-U75V).

5.2 Recomndation

As it is said and analyzed before, the wheel-rail contact of (AS4140-V1657) and (C74&U75V) material compositions is enhanced by strength and cost respectively than that of wheel -rail contact (CL60- U71MN). So it's better for Ethiopian Railway Corporation to use this wheel rail contact (AS4140&V1657) for the national railway system by making further study

5.3 Future Works

In this paper the stress caused by vertical load and thermal stress of three different wheel and rail contact materials are studied. the future work proposed by the end of this work for the improvement good contact of the wheel and rail , can be summarized in the following points

- Influences of different braking systems on rail -wheel contact damage
- Influences different environmental contact (dry, wet, and oily) on wheel/rail

References

[1] Smith, J. O. and Liu, C. K.: Stresses due to tangential and normal loads on an elastic solid with application to some contact stress problem, *J. Appl. Mech.*, 20,157–166, 1953.

[2] Haines, D. J. and Ollerton, E.: Contact stress distribution on elliptical contact surfaces subjected to radial and tangential forces, *Proc. of Inst. of Mechanical Engi-neers*, London, 177(4), 45–54, 1963.

[3] Sack_eld, A. and Hills, D. A.: Some useful results in the classical Hertz contact problem, *Journal of Strain Analysis*, London, 18(2), 101–105, 1983

[4] Z. Li. Wheel-Rail Contact and Its Application to Wear Simulation. Doctoral Thesis proposal, Delft university of Technology, (2002). ISBN 90-407-2281-1.

[5] R. Enblom. On simulation of uniform wear and profile evolution in the wheel-rail contact, Doctoral Thesis KTH, Stockholm, Sweden (2006).

[6] R. Roberti, S. Bruni. Development of operations of tilting train on Italian network, Proceedings 5th World Congress on Railway Research, Koln, Germany, 25-29, (2001).

[7] A. H. Wickens. Fundamentals of Rail Vehicle Dynamics, Swets and Zeitlinger, Lisse, the Netherlands (2003

[8] T. Matsudaira, Dynamics of High Speed Rolling Stock, JapaneseNational Railways RTRI Quarterly Reports, Special Issue, 1963.

[9] H. Hertz, On The Contact of two Elastic Solids, London:Macmillan & Co. Cap. 5, 1896, pp. 146-162

[10] S. Soemantri, W. Puja, B. Budiwantoro, M. Parwata, D. J.Schipper, Solution to Hertzian contact problem between Wheeland Rail for small radius of curvature, JSME, 4, 2010, pp. 669-677.

[11] A. Ekberg, E. Kabo, H. Andersson, An engineering model for prediction of rolling contact fatigue of railway wheels, Fatigue& Fracture of Engineering Materials & Structures, 25 (2002) 899-909

[12] K. Dang Van, M. Maitournam, Z. Moumni, F. Roger, Comprehensive approach for modeling fatigue and fracture of rails ,Engineering Fracture Mechanics, 76 (2009) 2626-2636

[13] M. A. Tanvir, "Temperature rise due to slip between wheel and rail—an analytical solutionfor hertzian contact," Wear, vol. 61, no. 2, pp. 295–308, Jun. 1980

[14] K. Knothe and S. Liebelt, "Determination of temperatures for sliding contact with applications for wheel-rail systems," Wear, vol. 189, no. 1–2, pp. 91–99, Oct. 1995

[15] M. Ertz and K. Knothe, “A comparison of analytical and numerical methods for the Calculation of temperatures in wheel/rail contact,” Wear, vol. 253, no. 3–4, pp. 498–508,Aug. 2002.

[16] V. Gupta, G. T. Hahn, P. C. Bastias, and C. A. Rubin, “Calculations of the frictional Heating of a locomotive wheel attending rolling plus sliding,” Wear, vol. 191, no. 1–2, pp.237–241, Jan. 1996.

[17] M. Spiryagin, K. S. Lee, H. H. Yoo, O. Kashura, and S. Popov, “Numerical calculation of temperature in the wheel–rail flange contact and implications for lubricant choice,” Wear, vol. 268, no. 1–2, pp. 287–293, Jan. 2010.

[18] NannanZong, Manicka Dhanasekar Analysis of Rail Ends under Wheel Contact Loading International Journal of Mechanical, Aerospace, Industrial, Mechatronic and Manufacturing Engineering Vol:6, No:8, 2012

[19] Carbon steel Wikipedia the free encyclopedia

[20] Tribological properties of tyre steel in rolling-sliding contact against bainitic rail steel

[21] T672 Wheel Steel Handbook Final

[22] T672 Wheel Steel Handbook Final railsafty &standards board

[23] www.buau.com.au 4140 High tensile

[24] Mingru Zhang and Haicheng Gu, Microstructure and mechanical properties ofrailway wheels manufactured with low-medium carbon Si-Mn-Mo-V steel,Journal of University of Science and Technology Beijing Volume 15, Number 2,April 2008

[25] List of thermal conductivity Wikipedia

[26] European Committee for Standardization, Railway applications - Track - Rail - Part 1: Vignole railway rails 46 kg/m and above, EN 13674-1:2011

[24] Esveld C. (2001), Modern Railway Track, 2nd edition, MRT-Productions, The Netherlands

[25] National Standards of the People's Republic of China (GB 2585—2007

[26] H.K.D.H. Bhadeshia and R.W.K. Honeycombe, Steels - Microstructure and properties,

2006, ISBN 978-0-750-68084-4

[27] T. C. Kennedy, C. Plengsaard, and R. F. Harder, “Transient heat partition factor for a

Sliding railcar wheel,” Wear, vol. 261, no. 7–8, pp. 932–936, Oct. 2006

[27] cost of wheel rail alibaba stock

[28] South-north Line and East-west Line (Phase I) Light Rail EPC Project of Addis Ababa, Ethiopia, Technical Specifications of Vehicles, China Railway Group (CRECG) Project Manager Office for Light Rail Project of Ethiopia, July 2013

[29] Jabbar{Ali Zakeri, Masoud Fathali and Nima Boloukian Roudsari: Effectsof Rail Cant on Wheel–Rail Contact Forces in Slab Tracks, *International Journal of Mechanics and Applications*, 1(1), 12–21, 2011.

[30] Zong, N. and Dhanasekar, M.: Analysis of Rail Ends under Wheel Contact Loading, *International Journal of Aerospace and Mechanical Engineering*, 6, 452–460,2012.

[31] Zhu, J. J., Ahmed, A. K. W. and Rakheja, S.: An Adaptive Contact Model forsimulation of Wheel–rail Impact Load due to a Wheel Flat, 13*th National Conferenceon Mechanisms and Machines*, IISc, Bangalore, India, 12–13, 2007.

[32] Mehmet Ali Arslan and Oguz Kayabasi: 3–D Rail–Wheel contact analysis usingFEA, *Advances in Engineering Software*, 45, 325–331, 2012.

[33] Pramod Murali Mohan: Analysis of Railway Wheel to study Thermal and Structural Behaviour, *International Journal of Scienti_c & Engineering Research*, 3(11),2012

[34] Vahid Monfared: Contact Stress Analysis in Rolling Bodies by Finite ElementMethod (FEM) Statically, *Journal of Mechanical Engineering and Automation*, 2(2),12–16, 2012